Geoscience Frontiers 5 (2014) 711–727

Contents lists available at ScienceDirect

China University of Geosciences (Beijing)

Geoscience Frontiers

journal homepage: www.elsevier.com/locate/gsf

Research paper

Alkali control of high-grade metamorphism and granitization

Oleg G. Safonov [a,c,d,*], Leonid Y. Aranovich [b,d]

[a] Institute of Experimental Mineralogy RAS, Chernogolovka, Moscow Region, Russia
[b] Institute of Geology of Ore Deposits, Petrography, Mineralogy and Geochemistry RAS, Moscow, Russia
[c] Department of Petrology, Moscow State University, Moscow, Russia
[d] Department of Geology, University of Johannesburg, Johannesburg, South Africa

ARTICLE INFO

Article history:
Received 11 October 2013
Received in revised form
27 February 2014
Accepted 14 March 2014
Available online 5 April 2014

Keywords:
High-grade metamorphism
Alkali activity
Fluids
Reaction textures
Fluid–mineral reactions
Thermodynamic modeling

ABSTRACT

We review petrologic observations of reaction textures from high-grade rocks that suggest the passage of fluids with variable alkali activities. Development of these reaction textures is accompanied by regular compositional variations in plagioclase, pyroxenes, biotite, amphibole and garnet. The textures are interpreted in terms of exchange and net-transfer reactions controlled by the K and Na activities in the fluids. On the regional scale, these reactions operate in granitized, charnockitized, syenitized etc. shear zones within high-grade complexes. Thermodynamic calculations in simple chemical systems show that changes in mineral assemblages, including the transition from the hydrous to the anhydrous ones, may occur at constant pressure and temperature due only to variations in the H_2O and the alkali activities. A simple procedure for estimating the activity of the two major alkali oxides, K_2O and Na_2O, is implemented in the TWQ software. Examples of calculations are presented for well-documented dehydration zones from South Africa, southern India, and Sri Lanka. The calculations have revealed two end-member regimes of alkalis during specific metamorphic processes: rock buffered, which is characteristic for the precursor rocks containing two feldspars, and fluid-buffered for the precursor rocks without K-feldspar. The observed reaction textures and the results of thermodynamic modeling are compared with the results of available experimental studies on the interaction of the alkali chloride and carbonate-bearing fluids with metamorphic rocks at mid-crustal conditions. The experiments show the complex effect of alkali activities in the fluid phase on the mineral assemblages. Both thermodynamic calculations and experiments closely reproduce paragenetic relations theoretically predicted by D.S. Korzhinskii in the 1940s.

1. Introduction

Traditionally, pressure (P) and temperature (T), and partial pressure (fugacity) of some volatile components (H_2O, CO_2, O_2) have been considered as the major intensive variables controlling metamorphic mineral assemblages in rocks of fixed bulk composition (e.g. Spear, 1993). On the basis of paragenetic analysis of rocks from the Precambrian high-grade metamorphic rocks and granitoids of the eastern Siberian region, Korzhinskii (1946, 1962) developed a concept of "mobility of alkalis during metamorphism and granite formation". According to this concept, chemical potentials of K and Na may be just as important factor and can be considered as intensive variables, as well. Applying this concept Korzhinskii (1946) proposed a number of mineralogical criteria to evaluate the influence of alkali activities in melts and fluids on mineral assemblages from granitic and syenitic rocks. Later, Korzhinskii (1962) concluded that the formation of the orthopyroxene-K-feldspar assemblages after metapelitic gneisses (termed as "charnockitization") should also be considered as an example of a process controlled by alkali activities in fluids.

Similar to T, P, H_2O activity, and other conventional intensive variables in metamorphic systems, the variations of alkali activities in fluids should be recorded in the regular changes in mineral

* Corresponding author. Institute of Experimental Mineralogy RAS, Chernogolovka 142432, Moscow Region, Russia.
E-mail address: oleg@iem.ac.ru (O.G. Safonov).

Peer-review under responsibility of China University of Geosciences (Beijing)

Production and hosting by Elsevier

1674-9871/$ – see front matter © 2014, China University of Geosciences (Beijing) and Peking University. Production and hosting by Elsevier B.V. All rights reserved.
http://dx.doi.org/10.1016/j.gsf.2014.03.010

assemblages, zoning of minerals and reaction textures involving K and/or Na-bearing phases, and, correspondingly, expressed in mineral reactions controlled by those activities. Perchuk and Gerya (1993) applied Korzhinskii's alkali mobility concept to explain textural features and regular compositional trends in coexisting biotite, orthopyroxene and plagioclase related to the development of the K-feldspar micro-veins in charnockitic gneisses and charnockites from central Finland and SW Baikal. Since then, similar textural and compositional relations have been repeatedly reported in granulites from many high-grade terrains (Hansen et al., 1995; Franz and Harlov, 1998; Harlov et al., 1998; Newton et al., 1998; Harlov and Wirth, 2000; Perchuk et al., 2000; Harlov and Förster, 2002; Montanini and Harlov, 2006; Touret and Huizenga, 2011; Rajesh et al., 2013). These findings have become a basis for a new approach, which invokes complex, poly-ionic aqueous solutions and brines as a factor of high-grade metamorphism (Newton, 1995; Aranovich and Newton, 1996; Newton et al., 1998; Yardley and Graham, 2002; Newton and Manning, 2010; Touret and Nijland, 2013).

The present paper reviews typical examples of reaction textures, which reflect the passage of fluids with variable alkali activities. It then considers the possible fluid-mineral reactions responsible for the development of these textures and for the accompanying compositional variations in the compositions of the coexisting minerals. These reactions are then thermodynamically modeled in simple chemical systems under variable alkali and H_2O activities and quantitative estimates of alkali activities presented for a few well documented examples of fluid-rock interaction in intermediate metamorphic rocks and metapelites.

Mineral and end-member abbreviations: Ab – albite, Alm – almandine, Amph – amphibole, An – anorthite, Ann – annite, Ap – apatite, Bar – baroasite, Bt – biotite, Cpx – clinopyroxene, Di – diopside, Eas – eastonite, Ed – edenite, En – enstatite, Fs – ferrosillite, Grs – grossular, Grt – garnet, Hbl – hornblende, Hed – hedenbergite, Ilm – ilmenite, Kfs – K-feldspar, Kls – kalsilite, Mt – magnetite, Ol – olivine, Opx – orthopyroxene, Or – orthoclase, Phl – phlogopite, Pl – plagioclase, Prg – pargasite, Prp – pyrope, Qtz – quartz, Sid – siderophillite, Sph – sphene, Tr – tremolite, Ts – tschermackite, Win – winchite

2. Mineralogical criteria and reactions indicative of variable alkali activities

2.1. Reactions involving feldspars only

Fig. 1 shows the pronounced dependence of the alkali feldspar K content on the K/Na ratio in a coexisting alkali chloride brine at 900 °C and 1000 MPa according to experimental data by Aranovich et al. (2013). In this example, the K/(K + Na) ratio of the coexisting phases is defined by a very well known exchange reaction (Orville, 1963; Iiyama, 1965):

$$\mathrm{Ab} + \mathrm{KCl} = \mathrm{Kfs} + \mathrm{NaCl} \quad (1)$$

Even though conditions at 900 °C are considerably super-solvus in the alkali feldspar system (Yund and Tullis, 1983), the behavior is very similar to the alkali feldspar–brine equilibria at lower temperatures. Thus, very orthoclase-rich alkali feldspars can coexist with a relatively Na-rich aqueous chloride fluid. Slight shifts in the fluid K/(K + Na) ratio (from 0.2 to 0.3) result in large changes in feldspar composition (from Kfs_{20} to Kfs_{80}), as emphasized by Orville (1963). This mode of K-enrichment in rocks is much more effective than could result from a fluid-undersaturated partial melting of mica- and/or amphibole-bearing rocks (Aranovich et al., 2013).

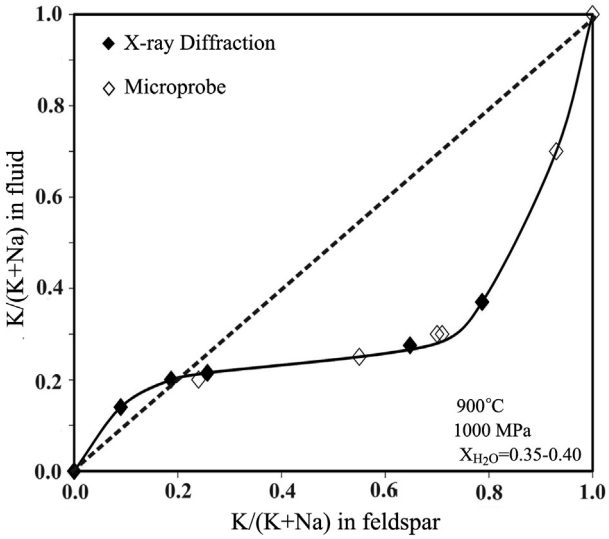

Figure 1. K-Na exchange between alkali feldspar and a KCl-NaCl brine according to the experimental data by Aranovich et al. (2013).

Reaction (1) can be re-written without specifying particular alkali species in the fluid as:

$$\mathrm{Ab} + 0.5\ \mathrm{K_2O} = \mathrm{Kfs} + 0.5\ \mathrm{Na_2O} \quad (1a)$$

where K_2O and Na_2O refer to the (virtual) solid oxides in the rock under consideration. This reaction indicates that the K/Na ratio in alkali feldspars may provide an estimate of the a_{K_2O}/a_{Na_2O} ratio in the rock and, correspondingly, in the coexisting fluid phase. Korzhinskii (1946) suggested that variations in the K_2O and Na_2O chemical potentials (activities) should also affect the composition of plagioclase coexisting with alkali feldspar. He proposed a criterion: *the higher the anorthite content of plagioclase coexisting with K-feldspar, the higher the K activity corresponding to this assemblage* due to the reaction

$$n\mathrm{An}(1-n)\mathrm{Ab} + 0.5m\mathrm{K_2O} = (1-n-m)\ \mathrm{Ab}m\mathrm{Or} + n\mathrm{CaO} + 0.5m\mathrm{Na_2O} \quad (2)$$

In two-feldspar assemblages, this reaction simultaneously operates with reaction (1a), indicating that an increase in the K_2O activity should produce an assemblage of more anorthite-rich plagioclase with orthoclase-rich alkali feldspar. Fig. 2 illustrates these relations in terms of the $\log(K^+/H^+)$ and $\log(Na^+/H^+)$ ratios after Perchuk et al. (2000).

Reaction textures of plagioclase replacement by K-feldspar are common for granitic rocks, and they are usually interpreted as products of sub-solidus interaction of the plagioclase with post-magmatic fluids (Eskola, 1956; Orville, 1962; Putnis et al., 2007). Perchuk and co-authors (Perchuk and Gerya, 1992, 1993; Perchuk et al., 1994) demonstrated textural evidence of the Korzhinskii's reaction (2) specifically for metamorphic rocks, i.e. the charnockitized gneisses of the Sulkava complex (Central Finland) and the Sharyzhalgay complex (SW Baikal). Here alkali feldspar rims and micro-veins occur along the plagioclase grain boundaries in contact with both quartz and Fe-Mg minerals. They found that the anorthite content of the plagioclase in contact with the micro-veins increased in accordance with reaction (2), while the orthoclase content of the alkali feldspar increases due to simultaneous reaction (1a). Subsequently, similar textural and compositional relations between plagioclase and K-feldspar have been described in

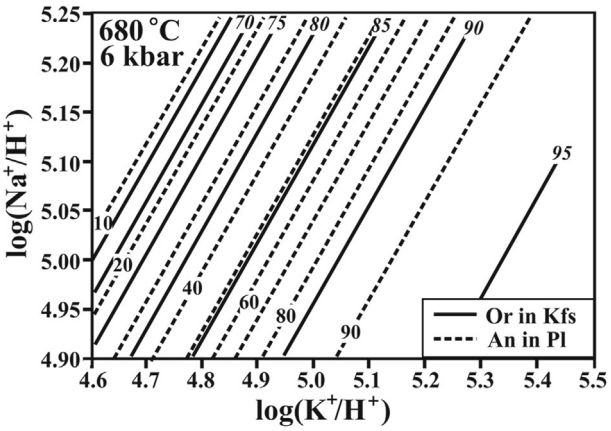

Figure 2. Compositional relations between coexisting alkali feldspar and plagioclase in terms of the $\log(K^+/H^+)$ and $\log(Na^+/H^+)$ activity ratios at 680 °C and 600 MPa illustrating Korzhinskii's reaction (2) operating simultaneously with exchange reaction (1). The computational method is described in Perchuk et al. (2000).

granulites from a number of high-grade terrains (Hansen et al., 1995; Franz and Harlov, 1998; Harlov et al., 1998; Harlov and Wirth, 2000; Harlov and Förster, 2002; Montanini and Harlov, 2006; Hansen and Harlov, 2007; Touret and Huizenga, 2011; Rajesh et al., 2013) (Fig. 3a–d). In most cases K-feldspar micro-veins form between plagioclase and quartz (Fig. 3a–d), suggesting a leading role for free silica in the formation of the micro-veins. Nevertheless, their appearance between plagioclase and Fe-Mg minerals (biotite, amphibole, pyroxenes, garnet) is also common in rocks of trondhjemitic to granitic composition. In some cases, the Fe-Mg minerals show clear reaction relations with the K-feldspar micro-veins, which are reflected in their zoning and/or decomposition (see below). The anorthite content of plagioclase, rimmed by the micro-veins, usually increases by not more than 5–7 mol.% (Perchuk and Gerya, 1993; Harlov and Wirth, 2000; Harlov and Förster, 2002; Hansen et al., 1995; Touret and Huizenga, 2011; Rajesh et al., 2013). However, extreme variations in the anorthite content of plagioclase (from 46 to 78 mol.% An) accompanying the formation of K-feldspar veins in charno-enderbites of the Mirny Station area in Antarctica were described by Parfenova and Guseva (2000). Newton (1995) proposed that the increase of the anorthite content in coexisting plagioclase should be considered as a true evidence for metasomatic origin of the K-feldspar micro-veins, rather than their crystallization from the interstitial granitic melt. The elevated BaO content of the K-feldspar, often documented in micro-veins (e.g., Hansen et al., 1995; Franz and Harlov, 1998; Harlov and Wirth, 2000), is also indicative of their metasomatic origin. Detailed BSE and TEM study of the micro-veins from granulites of the Ivrea-Verbano Zone (northern Italy) confirmed that such micro-veins could be produced metasomatically at temperatures above 500–600 °C via interaction with fluids of low H_2O activity (Harlov and Wirth, 2000).

Reaction (2) is not the only mechanism for the development of the K-feldspar micro-veins. Perchuk et al. (2000) suggested that they could also form during decomposition of plagioclase via the

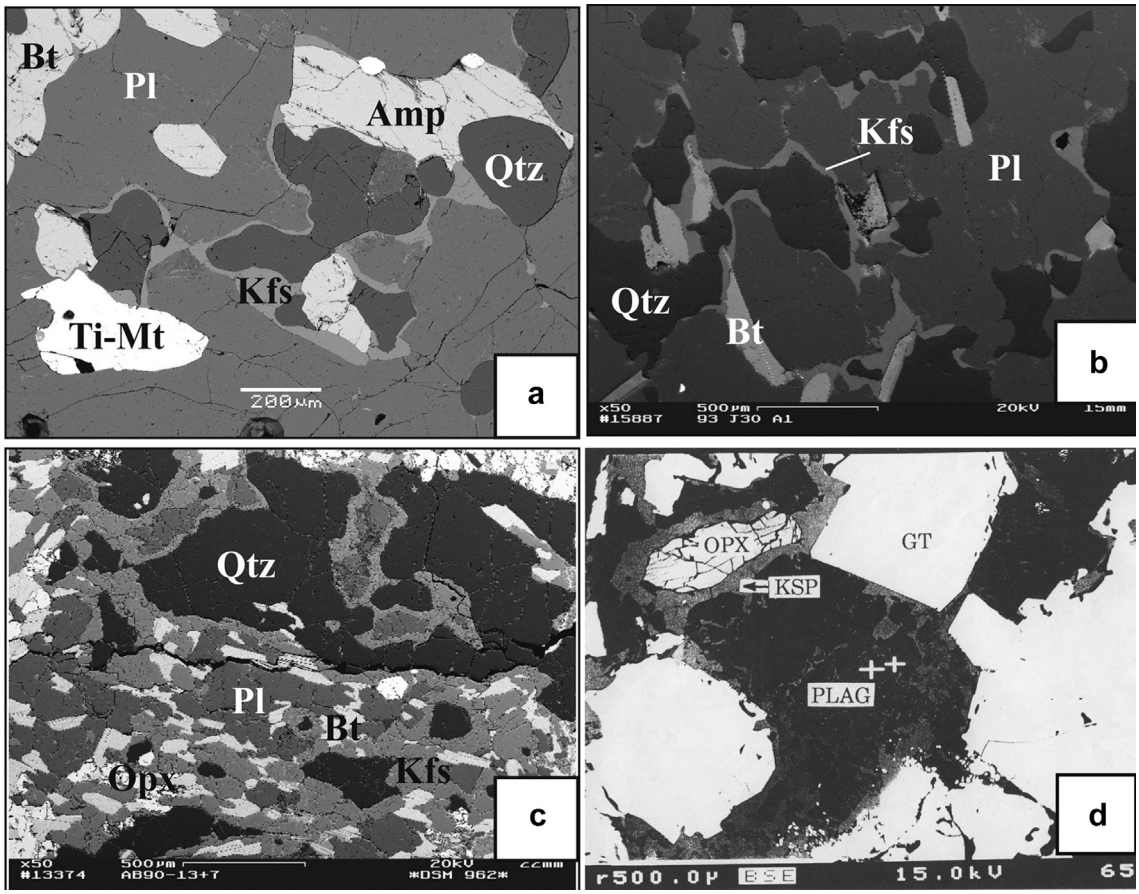

Figure 3. Back scattered electron (BSE) images of K-feldspar micro-veins at the contact between plagioclase and diverse minerals in granulite and upper-amphibolite rocks. (a) Biotite-hornblende tonalite gneiss from the Sand River, Limpopo Complex, South Africa (Safonov et al., 2012; Rajesh et al., 2013); (b) biotite tonalite gneiss from the Shevaroy Hills, southern India (Hansen and Harlov, 2007); (c) biotite-orthopyroxene gneiss from Seward Peninsular, Alaska (Harlov and Förster, 2002); (d) garnet-bearing charnockite gneiss from Shevaroy Hills, southern India (Hansen et al., 1995).

net-transfer reaction that involves, in addition to K_2O and Na_2O, variations in the CaO activity:

$$n\text{An}(1-n)\text{Ab} + 4n\text{Qtz} + 0.5(m+2n)\text{K}_2\text{O} = (1-n-m)\text{Ab}(m+2n)\text{Or} + (n\text{CaO} + 0.5m\text{Na}_2\text{O}) \quad (3)$$

Reaction (3) indicates that the higher the activity of K in the fluid, the more plagioclase is being replaced by K-feldspar with higher orthoclase content. At the same time the plagioclase composition may remain constant. Reaction (3) is a schematic representation of the dissolution/precipitation mechanism of feldspar-fluid reactions, which usually results in sharp contacts between initial and new phases, very weak compositional zoning in both phases, and common porosity in the newly formed rim (Labotka et al., 2004; Putnis et al., 2007; Putnis and Austrheim, 2013). The formation of K-feldspar micro-veins is sometimes followed by myrmeckitic plagioclase-quartz intergrowths forming via an inverse reaction (3) and represents consecutive stages of the mineral-fluid reactions (Harlov and Wirth, 2000; Perchuk et al., 2000; Touret and Huizenga, 2011; Rajesh et al., 2013; Touret and Nijland, 2013). Harlov and Wirth (2000) documented albitic rims along the contacts of K-feldspar micro-veins with plagioclase and interpreted them as results of increase of Na_2O activity and a very low K/Na ratio (Fig. 1) in the supercritical brine fluid. Taking into account very rapid replacement of both plagioclase by K-feldspar (Orville, 1963; Labotka et al., 2004; Putnis et al., 2007) and K-feldspar by albite or sodic plagioclase (Norberg et al., 2011, 2013; Putnis and Austrheim, 2013), these relations show a strong buffering effect of reactions (1)–(3) on the K/Na activity ratio in fluids. Plagioclase reacting to form K-feldspar during interaction with a K-rich fluid consumes K and supplies Na (and Ca) into the fluid. When the K/Na activity ratio of the incoming fluid is low, the reverse reactions result in formation of albite or myrmeckites, leading to the increase of the K/Na ratio until the system is buffered. The buffering will be more rapid and efficient if the original assemblages interacting with the alkali-bearing fluid contain both plagioclase and K-feldspar. In this respect, it is worth noting that the K-feldspar micro-veins are most commonly observed and best developed in rocks originally devoid of K-feldspar.

Reactions (1)–(3) constrain the a_{K_2O}/a_{Na_2O} ratio, but do not allow for comparison of the individual alkali activity values for various mineral assemblages containing alkali feldspars. Such a comparison requires considering additional net-transfer reactions involving either K_2O or Na_2O or both.

2.2. Reactions involving Fe-Mg minerals

On the basis of the Schreinemakers analysis of the system CaO-(Mg, Fe)O-Al_2O_3-SiO_2, involving biotite, hornblende, clinopyroxene, plagioclase, K-feldspar, quartz, and magnetite in terms of $\mu_{K_2O}-\mu_{Na_2O}$ (Fig. 4), Korzhinskii (1946) showed that variations of K_2O and Na_2O activities in the fluids and/or melts can be an important factor for the diversity of mineral parageneses of granitoid rocks at constant temperature, pressure, and H_2O activity. He proposed criteria which allow for the comparison between the relative alkali activity during formation of granitoid parageneses (Korzhinskii, 1946): *(1) the more "basic" (i.e. with less polymerized structure) and the "higher the temperature" Fe-Mg (alumino)silicate that coexists with K-feldspar, the higher the K activity corresponding to this assemblage; and (2) the more "basic" and the "higher the temperature" Fe-Mg (alumino)silicate that coexists with sodic plagioclase, the higher the Na activity corresponding to this assemblage.* Fig. 4 shows that K-feldspar coexists with biotite at a low μ_{K_2O} (field I). With increasing μ_{K_2O} in the coexisting fluid or melt at constant μ_{Na_2O} (for example, above invariant point A), K-feldspar becomes stable with biotite + hornblende (field II), biotite + hornblende + clinopyroxene (field III), and, finally, with biotite + clinopyroxene (field IV). Field III is subdivided into two regions by the reaction (Qtz) indicating the stability of syenitic quartz-free assemblages at high μ_{K_2O} and suggesting that an increase in the alkali activity results in the consumption of free silica. Increase of μ_{Na_2O} from the field IV (on the right hand side of point A) consequently stabilizes assemblages of hornblende with K-feldspar (field III), hornblende with K-feldspar and sodic plagioclase (field II) and hornblende with sodic plagioclase (field I).

The above relations agree well for granitoid rocks. Normal granites and granodiorites usually do not contain clinopyroxene. This mineral appears in the alkaline granitoids (especially in their relatively iron-rich varieties, A-type granites, rappakivi, etc.), where K-feldspar usually predominates over plagioclase. Clinopyroxene becomes a common mineral in syenites and quartz syenites of higher alkalinity in comparison to granites. Fig. 5a shows an example of the clinopyroxene-K-feldspar (+sphene) assemblage from the Madiapala syenite, Limpopo Complex, South Africa. According to Fig. 4 this assemblage corresponds to the highest chemical potential of K_2O in the melt or fluid. An increase in the Na_2O chemical potential transforms this assemblage to the assemblage of pargasite-edenite amphibole, with an Na/(K + Na) ratio of about 0.7, and almost pure albite (Fig. 5b) in direct accordance with the relations in Fig. 4.

Clinopyroxene-K-feldspar assemblages are relatively rare in metamorphic rocks, although this paragenesis has been documented in some gneissic terrains (Harlov et al., 2006; Hansen and Harlov, 2007; Harlov, 2012; Safonov et al., 2012; Rajesh et al., 2013). In most cases, it is developed in the vicinity of charnockitic or charno-enderbitic veins cross cutting biotite- and hornblende-bearing gneisses, suggesting that formation of this assemblage is related to fluids expelled from magmas of granitic composition. Fig. 6a shows an example of a clinopyroxene-K-feldspar reaction texture locally developed in amphibole-biotite gneiss (Sand River gneiss) cross cut with charno-enderbite veins at the Causeway locality, Limpopo Complex, South Africa (Safonov et al., 2012; Rajesh et al., 2013). The formation of the clinopyroxene-K-feldspar assemblage around biotite corresponds to an increase in the K_2O activity driving the reaction

$$\text{Bt} + 3\text{An (in Pl)} + 18\text{Qtz} + 3(\text{K}_2\text{O}) = 3\text{Cpx} + 7\text{Kfs} + (\text{H}_2\text{O}) \quad (4)$$

to the right. This reaction is analogous to the reaction (Hbl) in Fig. 4. Similar clinopyroxene-K-feldspar reaction textures were experimentally reproduced in experiments on the interaction of the Sand River gneiss with H_2O-CO_2-KCl fluids at 550 MPa and 750 and 800 °C (Safonov et al., 2012). Fig. 6b shows that decomposition of biotite in the gneiss to clinopyroxene + K-feldspar at 800 °C and $X_{KCl} = KCl/(KCl + H_2O + CO_2) = 0.03$ in the fluid is accompanied by extensive replacement of plagioclase with K-feldspar along grain boundaries and cracks. In addition, local partial melting with formation of a potassic melt is observed. In the experiments at 800 °C, the clinopyroxene-K-feldspar assemblage is observed only at $X_{KCl} > 0.01$ being replaced by the assemblages orthopyroxene + clinopyroxene and orthopyroxene + hornblende at lower concentrations of KCl. This proves that the clinopyroxene-K-feldspar assemblage corresponds to the highest activities of K_2O in the system in accordance with the diagram constructed by Korzhinskii (1946).

The diagram in Fig. 4 does not show reactions involving orthopyroxene and olivine, although these minerals are very important constituents of the alkali-rich granites and rocks of the charnockite series. In order to demonstrate the role of the K_2O activity in the origin of charnockite assemblages, Korzhinskii (1962) constructed the Schreinemakers diagram for the system (Mg, Fe)O-Al_2O_3-SiO_2

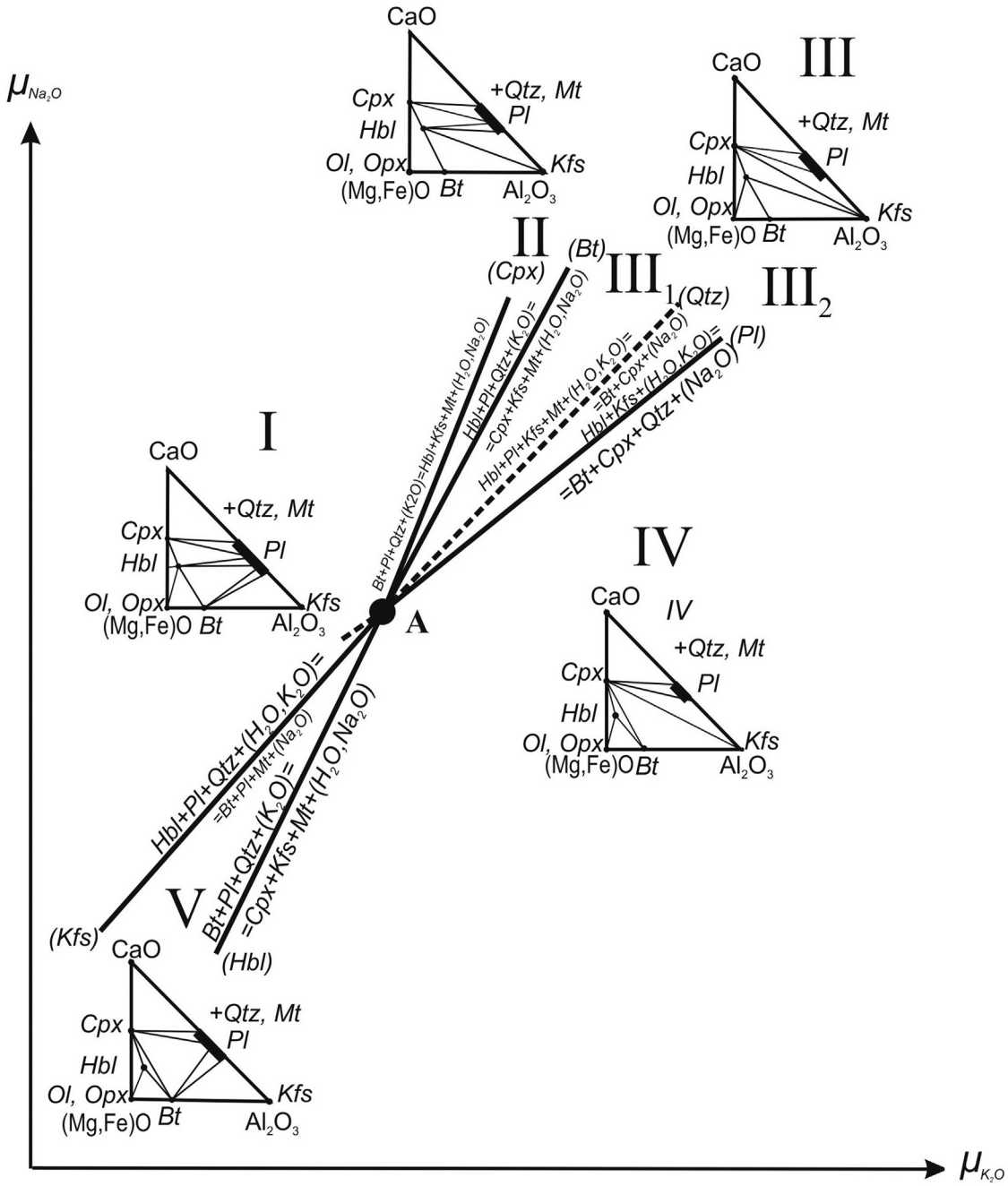

Figure 4. A Schreinemakers diagram showing variations for granitoid parageneses in the system CaO-(Mg, Fe)O-Al_2O_3-SiO_2 as a function of $\mu_{K_2O}-\mu_{Na_2O}$ after Korzhinskii (1946). I–IV indicate specific mineral assemblages discussed in the text.

in terms of $\mu_{K_2O}-\mu_{H_2O}$ (Fig. 7). This diagram visualizes that the assemblages Opx + Kfs and Ol + Kfs correspond to the highest chemical potential of K_2O. The above criteria by Korzhinskii (1946) are well fulfilled for this system as well since a high K_2O activity is reflected by the coexistence of Opx and Ol with K-feldspar. However in addition to the these criteria, the diagram (Fig. 7) allows for the introduction of a new mineralogical criterion for the high K_2O activity, i.e. *the less aluminous the (alumino)silicate that coexists with K-feldspar, the higher the K activity in the fluid.* In fact, the reaction

$$Al_2SiO_5 + 5Qtz + K_2O = 2Kfs \quad (5)$$

divides the diagram into two fields corresponding to sillimanite-(or kyanite)-bearing and sillimanite-free assemblages in quartz-saturated rocks. In the first of these fields, an increase of a_{K_2O} results in the formation of biotite in association with quartz and alumino-silicate. Reaction intergrowths of Bt + Qtz and Bt + Sil(Ky) + Qtz, which initially did not contain K-feldspar, are widely known in high-grade metamorphic rocks. Fig. 8a shows the replacement of cordierite by the Ti-free biotite and sillimanite in a tonalitic magma, which can be interpreted in terms of an increase in both the H_2O and K_2O activity in the magma and/or in the coexisting fluid according to the reaction:

$$3/2Crd + 1/2K_2O + H_2O = Bt + 5/2Sil + 2Qtz \quad (6)$$

Reactions of cordierite (and other Al-rich silicates) to biotite can easily be reproduced experimentally. Fig. 8b shows fringes of

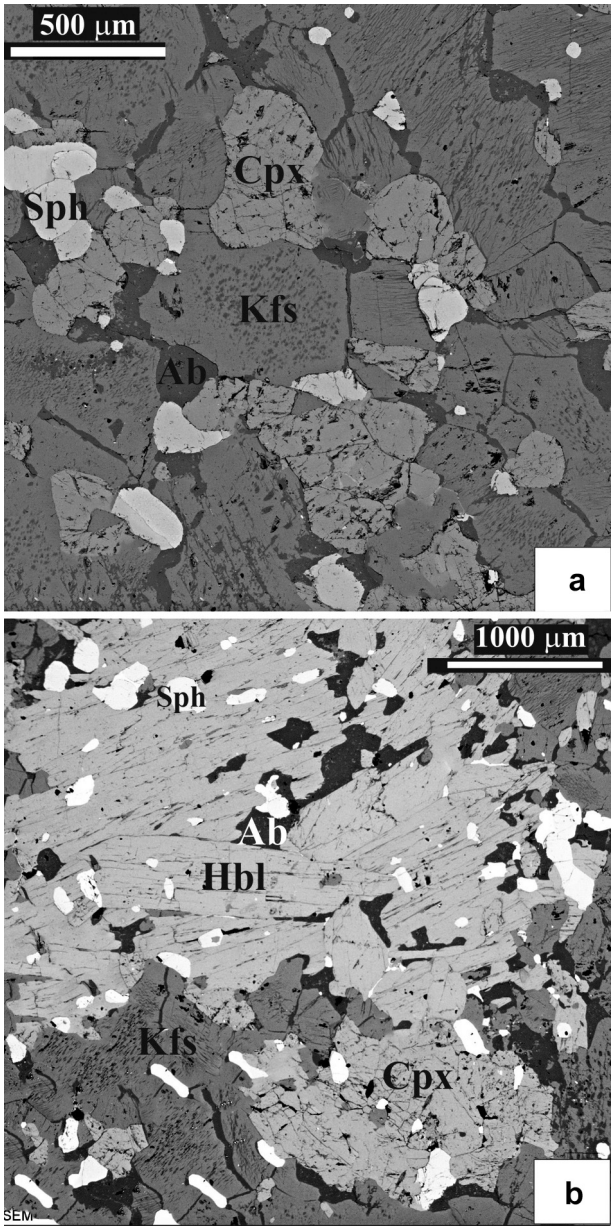

Figure 5. Relationship of alkali feldspars with clinopyroxene and amphibole in the Madiapala syenite (Limpopo Complex, South Africa). (a) The early clinopyroxene-K-feldspar (+sphene) assemblage indicating high K_2O activity according to the diagram (4); (b) replacement of the clinopyroxene by edenite-pargasite amphibole and K-feldspar by albite, which, according to the diagram (4), suggests an increase of the Na_2O activity at later stages of the rock evolution.

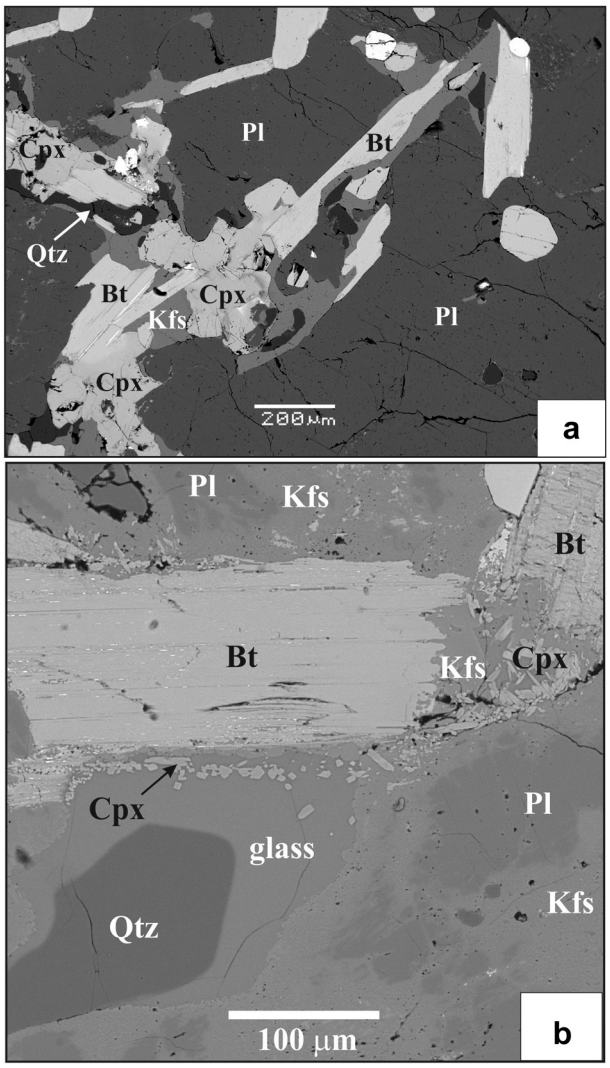

Figure 6. Formation of a clinopyroxene-K-feldspar assemblage during decomposition of biotite interacted with the fluids of high K_2O activity. (a) Clinopyroxene-K-feldspar assemblage associated with a partially dehydrated biotite-hornblende gneiss from the Causeway locality, Limpopo Complex, South Africa, formed via reaction (4) due to an increase in the K_2O activity in the fluid (Safonov et al., 2012; Rajesh et al., 2013); (b) experimentally reproduced decomposition of biotite in a biotite-hornblende gneiss from the Causeway locality due to interaction with a H_2O-CO_2-KCl fluid at 550 MPa and 800 °C (Safonov et al., 2012).

biotite on cordierite in a metapelite that has interacted with a H_2O-CO_2-KCl fluid ($X_{KCl} = 0.025$) at 800 °C and 600 MPa. It is clearly seen that even relatively low concentrations of the K component in the fluid and, thus low K activity, is sufficient to produce biotite after cordierite.

At higher a_{K_2O}, alumino-silicates become unstable and are replaced by K-feldspar. Rims of K-feldspar around sillimanite in high-grade rocks were mentioned by Korzhinskii (1962). Rims of orthoclase and microperthite alkali feldspar around sillimanite and cordierite have been described by Korikovsky and Kislyakova (1975) in granulites from the Sutam Complex, Aldan Shield and were interpreted as a result of alkali input during granitization of the rocks. In the absence of alumino-silicate, cordierite decomposes to the assemblages Opx + Grt + Kfs (at low H_2O activity) or Grt + Bt + Kfs (at high H_2O activity) (Fig. 7). Subsequently, at low H_2O activity, Opx + Grt + Kfs breaks down to Ol + Kfs, i.e. the assemblage of an Al-free, Si-poor silicate with K-feldspar via the reaction:

$$Grt + 9Opx + K_2O = 6Ol + 2Kfs \quad (7)$$

At higher H_2O activities the charnockitic assemblage Opx + Bt + Kfs + Qtz is stable at high K_2O activities (Fig. 7). The model charnockitic reaction

$$Phl + 3Qtz = 3En + Kfs + H_2O \quad (8)$$

is independent of the K_2O activity. However, it has a gentle slope in Fig. 7 indicating dependence on both the K_2O and H_2O activities. Korzhinskii (1962) explained this apparent controversy as being

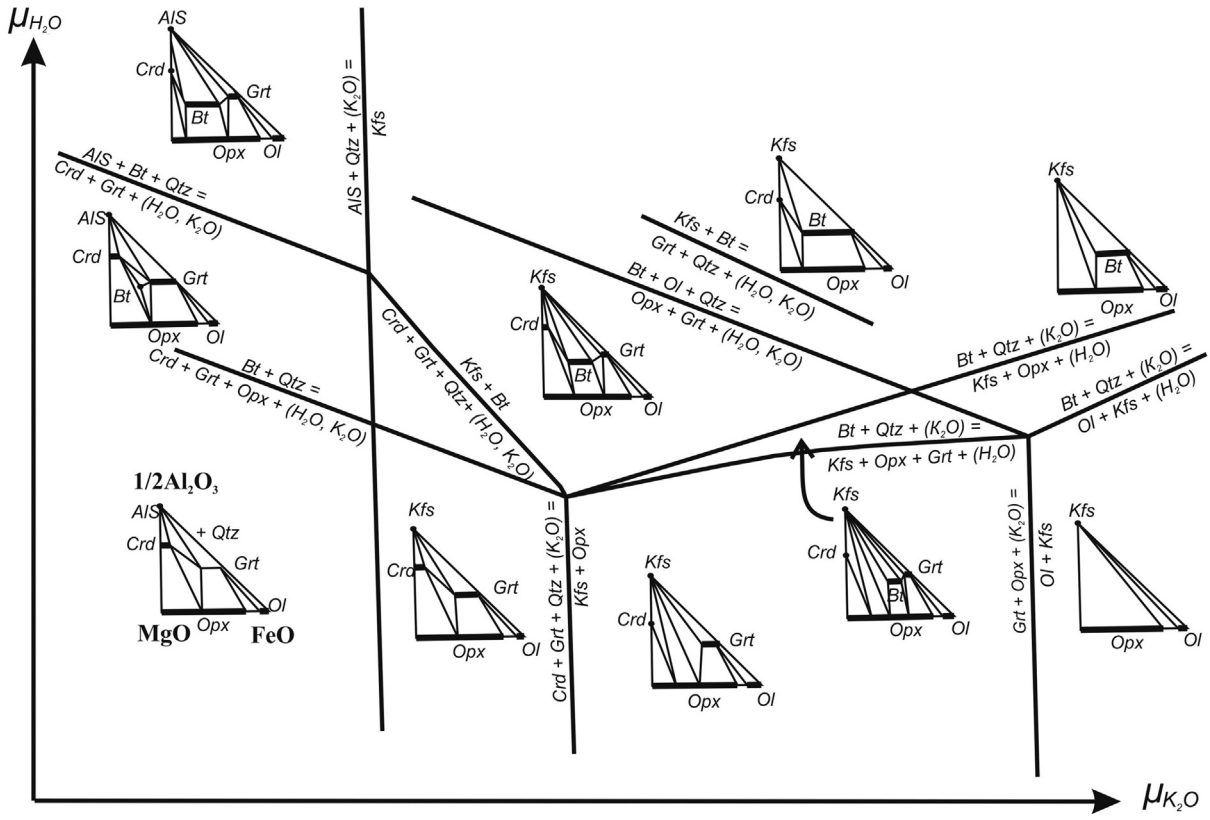

Figure 7. Schreinemakers diagram showing variations in parageneses for the system (Mg,Fe)O-Al_2O_3-SiO_2 as a function of $\mu_{K_2O}-\mu_{Na_2O}$, after Korzhinskii (1962).

due to the fact that the biotite composition in the charnockite assemblages does not lie exactly on the phlogopite-annite join but contains significant amounts of the eastonite-siderophillite end-members, while orthopyroxenes in these assemblages are usually Al-poor. On the basis of a detailed study of charnockitized gneisses from southern Finland and the Baikal region, Perchuk and co-authors (Perchuk and Gerya, 1992, 1993; Perchuk et al., 1994) concluded that the reaction

$$6(\text{Sid-Eas}) + 6\text{Qtz} + 3\text{K}_2\text{O} = 5(\text{Phl-Ann}) + 7\text{Kfs} + \text{H}_2\text{O} \quad (9)$$

operates simultaneously with reaction (8), what makes it dependent on the K_2O activity. They observed an inverse correlation between the Al-content in biotite and the anorthite content in coexisting plagioclase, reflecting that conjugate reactions (2) and (9) proceed via an increase in the K_2O activity. Parfenova and Guseva (2000) have observed a drop in Al_2O_3 content of 10 to 15 wt.% in biotite in contact with newly formed K-feldspar in charno-enderbites from the Mirny Station area in Antarctica and interpreted it as a result of reaction (9).

Perchuk and Gerya (1993) demonstrated that a decrease in the Al content also occurs in orthopyroxene and hornblende in contact with the K-feldspar micro-veins due to the reactions

$$(\text{Mg, Fe})\text{Al}_2\text{SiO}_6\ (\text{in Opx}) + 6\text{Qtz} + \text{K}_2\text{O} = \text{Opx} + 2\text{Kfs} \quad (10)$$

and

$$5\text{Prg} + 23\text{Qtz} + 3\text{K}_2\text{O} = 4\text{Ed} + \text{Ab} + 2\text{An} + 6\text{Kfs} + \text{H}_2\text{O} \quad (11)$$

Similar reactions can be re-written with Na_2O as the reactant and albite as the product. Reactions (9)–(11) allow addition of another criterion expressing an increase of alkali activity: the lower the Al content in the Fe-Mg mineral coexisting with K-feldspar (sodic plagioclase), the higher the K (Na) activity in the fluid.

However, this rule may be violated for tremolite-tschermackite-edenite-pargasite hornblendes, since the introduction of alkalis in these minerals is accompanied by isomorphism Ca + Mg = Na(K) + Al resulting in an increase in the Al-content of the mineral. Fig. 9a shows formation of hornblende (Hbl-2) after hornblende (HBl-1) in amphibolite from the Southern Marginal Zone of the Limpopo Complex (South Africa). Formation of Hbl-2 is accompanied by formation of K-feldspar reflecting an increase in the K_2O activity during crystallization of Hbl-2. In contrast to Hbl-1, which is rich in tremolite component and contains about 1 wt.% TiO_2, the composition of Hbl-2 is close to pargasite (see an insert in Fig. 9a) with about 0.5 wt.% TiO_2. These relations can be explained by the complex reaction

$$4/5\text{Tr (in Hbl)} + 21/5\text{Ab (in Pl)} + 2/5\text{An (in Pl)} + 1/5\text{H}_2\text{O} + \text{K}_2\text{O} = \text{Prg (in Hbl)} + \text{Kfs} + 8/5\text{Na}_2\text{O} + 39/5\text{Qtz} \quad (12)$$

showing that the Al content in hornblende depends on the a_{K_2O}/a_{Na_2O} ratio. This reaction proceeds along with the K-Na exchange reaction between the hornblende and the fluid. Notable increase in the K/(K + Na) ratio in Hbl-2 (0.29–0.35 compared to 0.15–0.16 in Hbl-1) supports this increase of a_{K_2O} in the fluid. In contrast to less than 0.01 wt.% Cl in Hbl-1, Hbl-2 contains 2.0–3.4 wt.% Cl suggesting an interaction with the KCl-rich fluid. Formation of similar Cl-rich potassic hornblende (1.5–2.3 wt.% Cl; K/(K + Na) = 0.48–0.57) after clinopyroxene and magnetite in a metasyenite from the Adirondack Complex (USA) is shown in Fig. 9b. Formation of the hornblende-K-feldspar assemblage after pyroxenes via an increase in the K activity can be described by several reactions involving pyroxenes and plagioclase, for example:

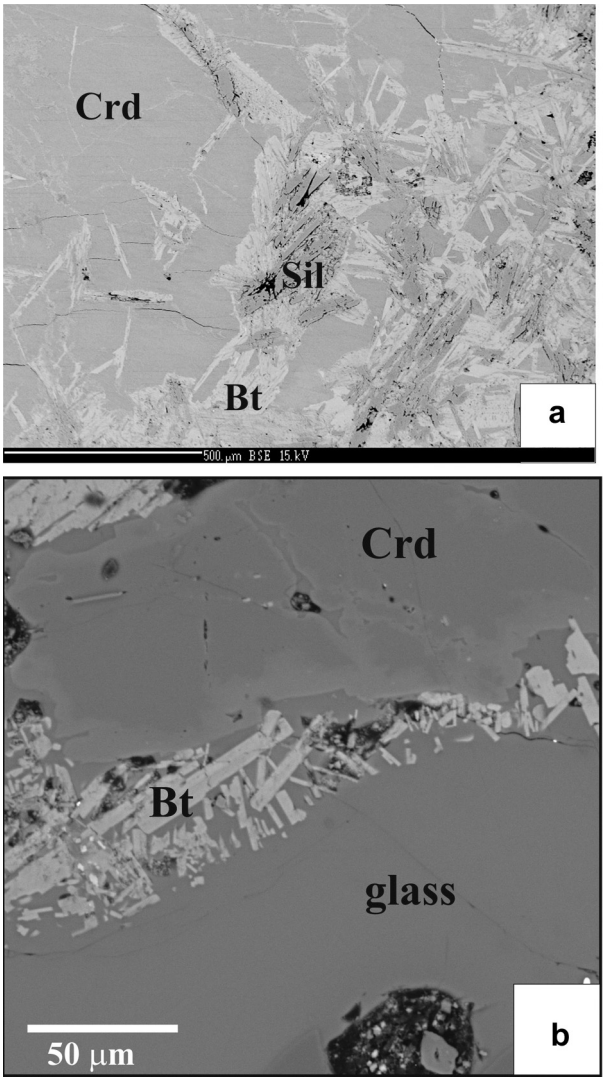

Figure 8. Cordierite reactions governed by an increase in the K_2O activity. (a) Replacement of relic cordierite entrapped by the tonalite melt with the assemblage biotite + sillimanite resulting from an increase in the alkali activity during crystallization of the melt, Petronella locality, Limpopo Complex, South Africa; (b) Fringes of biotite on cordierite produced during interaction of metapelite with a H_2O-CO_2-KCl fluid (X_{KCl} = 0.025) at 800 °C and 600 MPa. Light rims on cordierite are newly formed zones enriched in FeO.

$$19Opx + Cpx + 9An\ (in\ Pl) + 5Ab\ (in\ Pl) + 5H_2O + 4K_2O = 5Prg\ (in\ Hbl) + 8Kfs \quad (13)$$

Reaction (13) shows that, along with the formation of the K-feldspar micro-veins and blebs, crystallization of K-rich hornblende can be considered as indicative of increasing K_2O activity in metamorphic fluids. On the other hand, in most cases charnockitization and enderbitization of amphibolites provide the best examples of hornblende decomposition to the assemblages of two pyroxenes, plagioclase and K-feldspar (e.g. Korikovsky and Aranovich, 2010). Fig. 10 illustrates the local formation of such assemblage after hornblende in the orthopyroxene-bearing amphibolite from the Porya Bay Area, southern Kola Peninsula (Korikovsky and Aranovich, 2010), via the reaction:

$$Prg\ (in\ Hbl) + 9Qtz + K_2O = 2Opx + 2Cpx + 2Kfs + Ab + H_2O \quad (14)$$

Formation of incipient charnockites after biotite-hornblende tonalite gneisses documented in the rocks of Southern India, Sri Lanka and other Precambrian terrains (Janardhan et al., 1982; Hansen et al., 1984, 1987; Stähle et al., 1987; Burton and O'Nions, 1990; Perchuk et al., 2000; Rajesh et al., 2013) provides another example of the instability of hornblende during charnockitization as governed by alkali mobility (Perchuk et al., 2000). Hornblende can appear in the incipient charnockites as a phase related to the late stages of the charnockite evolution. Its development can be explained by reactions similar to (14) and, possibly, related to an increase in the Na activity of the fluids (Safonov et al., 2012; Rajesh et al., 2013).

Reaction (3) indicates the extraction of CaO from plagioclase into the fluid. However, this component can be also consumed during the formation of an additional Ca-rich phase such as clinopyroxene and grossular-rich garnet. The formation of clinopyroxene after biotite and plagioclase via reaction (4) is illustrated in Fig. 6a and b. In addition, Fig. 11 shows the relationship between clinopyroxene, orthopyroxene, and K-feldspar in a metamangerite from the Adirondack Complex (USA) (Safonov, 1998). Relationships between clinopyroxene, orthopyroxene, and plagioclase in the presence of K-feldspar and quartz are described by the reaction:

$$Opx + An\ (in\ Pl) + 5Qtz + (K_2O) = Cpx + 2Kfs \quad (15)$$

This reaction indicates that the assemblage Cpx + Kfs corresponds to a higher K_2O activity relative to the assemblage Opx + Kfs. From this point of view, formation of Cpx after Opx in the above example (Fig. 11) should correspond to an increase in K activity in the fluid during rock evolution. Distribution of these assemblages in the rocks could serve as an indicator of heterogeneity in the K activity in the mineral-forming fluids or melts. Two-pyroxene-bearing local-scale dehydration zones were documented in a number of gneissic terrains (Knudsen and Lidwin, 1996; Harlov et al., 2006; Harlov, 2012; Safonov et al., 2012; Rajesh et al., 2013). Regular distribution of orthopyroxene and clinopyroxene in rocks is also suggested for regional-scale amphibolite-to-granulite facies transition zones (Harlov and Förster, 2002; Hansen and Harlov, 2007). All these examples can be interpreted in terms of variations in alkali activities during dehydration processes. This conclusion is supported by experimental data on dehydration of tonalite gneisses under the influence of alkali chloride-bearing fluids (Harlov, 2004; Safonov et al., 2012). Safonov et al. (2012) found that the two-pyroxene-K-feldspar assemblage formed at lower concentrations of KCl in fluids, i.e. at lower activities of K compared to the clinopyroxene-K-feldspar assemblage, was in line with the displacement of equilibrium (15) to the right with increasing K_2O activity (Fig. 11).

Formation of grossular-rich garnet and K-feldspar after plagioclase, due to an increase in the K activity in a fluid corresponds to the reaction (Safonov, 1998):

$$An\ (in\ Pl) + 3Qtz + 2/3K_2O = 1/3Grs\ (in\ Grt) + 4/3Kfs \quad (17)$$

This reaction shows that the formation of K-feldspar micro-veins due to an increase in the K activity in a fluid, should be accompanied by an increase in the grossular content in the coexisting garnet or formation of new Ca-rich garnet. Fig. 12a shows the development of garnet containing 25 to 30 mol.% grossular in a K-feldspar-apatite vein cross cutting a large plagioclase crystal from a meta-anorthosite located in the Adirondack Complex, USA. The appearance of garnet and K-feldspar after plagioclase, and the increase in the Ca-content from the center to the rim of the garnet grains both indicate that the process was controlled by reaction (17), and occurred under varying (increasing) K_2O activity. Similar zonation of garnet has been described by Hansen et al. (1995) in the Shevaroy Hills

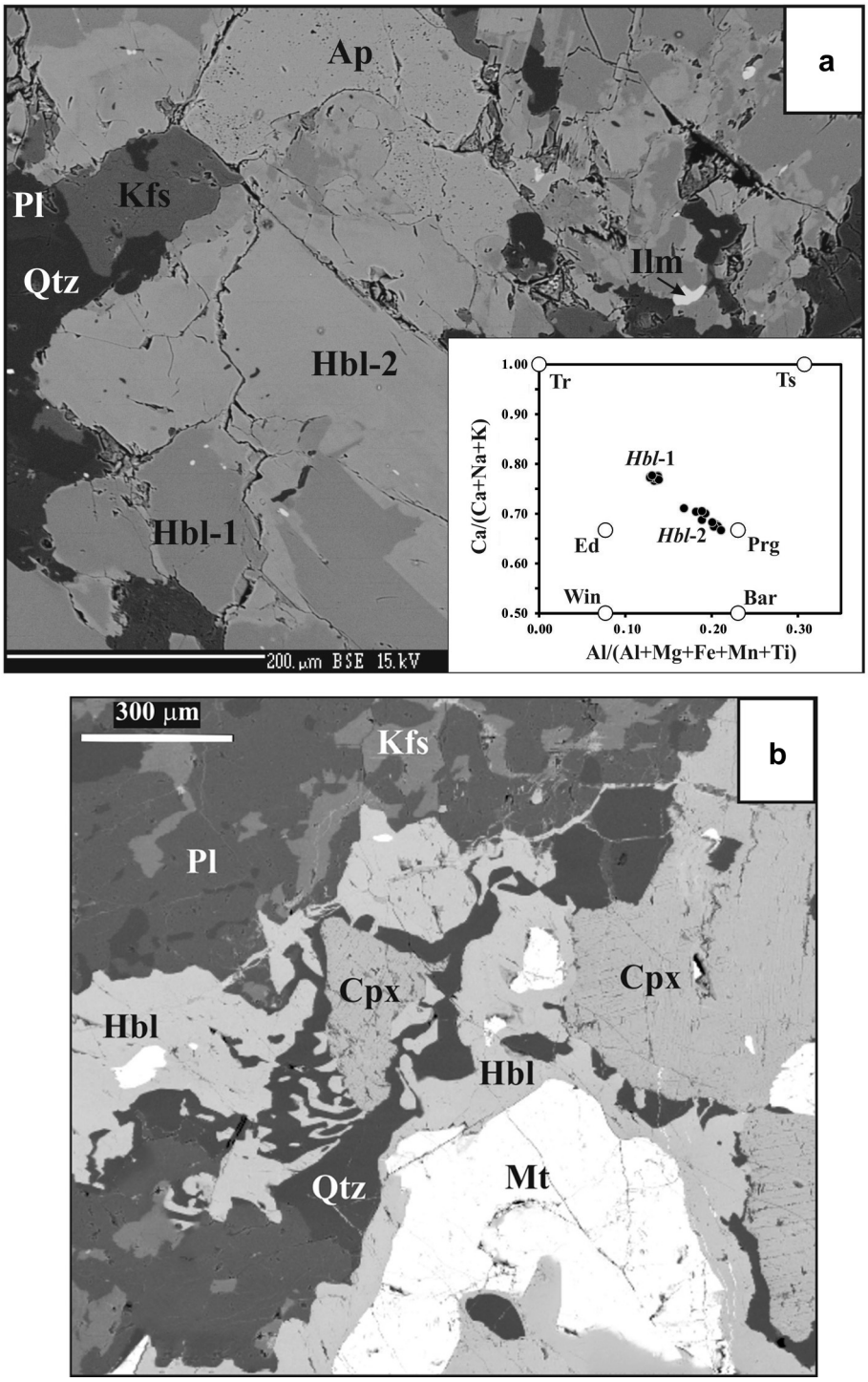

Figure 9. Hornblende as an indicator of an increase in alkali activity in fluids during high-grade metamorphism. (a) Formation of a new generation of Cl-rich potassic hornblende (Hbl-2) (+Ilm + Qtz) and K-feldspar after Cl-poor hornblende (Hbl-1) in amphibolite from the Southern Marginal Zone of the Limpopo Complex, South Africa. The inset shows differences in the composition of the primary and newly formed hornblende; (b) rims and symplectites of Cl-rich potassic hornblende around clinopyroxene and magnetite accompanied by K-feldspar micro-veins in a metasyenite from the Adirondack Complex, USA (Safonov, 1998).

charnockites, southern India (Fig. 3d). They noted that an increase in the grossular content in garnet towards the contact with K-feldspar micro-veins riming the garnet (Fig. 3d) is accompanied by an increase in the anorthite content in plagioclase and a decrease in the Al content in the coexisting orthopyroxene. These relations illustrate simultaneously operating reactions (17), (2), and (10) under increasing K activity in a fluid.

In experiments on the interaction of a biotite-hornblende gneiss with H_2O-CO_2-KCl fluids at 800 °C and 550 MPa Safonov et al. (2012) observed the formation of grossular-rich garnet during strong K-feldspatisation of the plagioclase (Fig. 12b). Garnet is associated with kalsilite, which is an additional proof for high K activity in the experiments. Reactions similar to (17) in which Na_2O replaces K_2O,

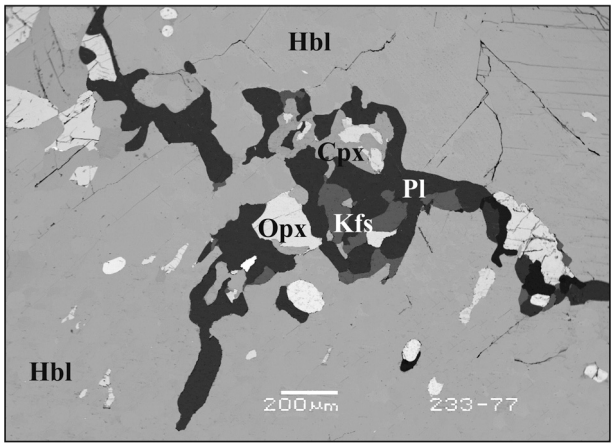

Figure 10. Local decomposition of hornblende to the assemblage orthopyroxene + clinopyroxene + plagioclase + K-feldspar resulting from an increase in the K_2O activity in the fluid (reaction 13) in an amphibolite from the Porya Bay Area, southern Kola Peninsula (Korikovsky and Aranovich, 2010).

$$An\ (in\ Pl) + 3Qtz + 2/3Na_2O = 1/3Grs\ (in\ Grt) + 4/3Ab\ (in\ Pl) \quad (17a)$$

garnet corona growth seems to be responsible for the formation of grossular-rich garnet after plagioclase in the experiments of Larikova and Zaraisky (2009). These authors showed that compared to pure H_2O, the 0.1 M NaCl aqueous solution provoked efficient garnet growth.

3. Thermodynamic modeling of the reactions depending on alkali activity

The Schreinemakers method applied by Korzhinskii (1946, 1962) allows for qualitative analysis of phase relations at arbitrary constant P, T, and a_{H_2O} under variable μ_{K_2O} and μ_{Na_2O} (Figs. 4 and 7). To be able to obtain information on the variations of these phase relations with temperature and pressure, the thermodynamic properties of mineral end-members and fluid species, including alkali components, must be introduced in the calculation

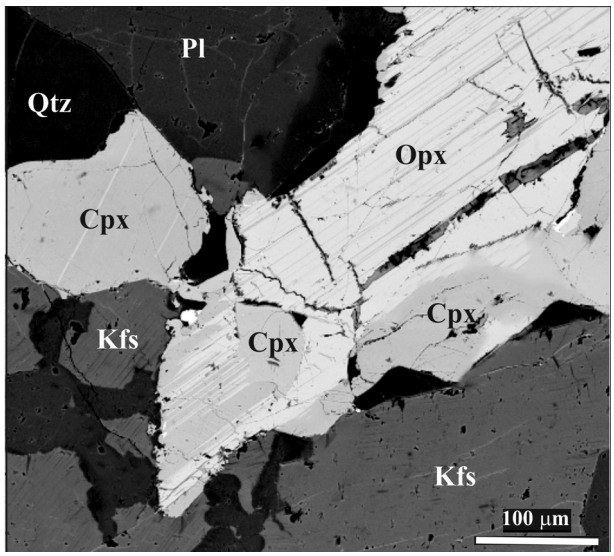

Figure 11. Replacement of orthopyroxene by clinopyroxene and K-feldspar governed via reaction (15) in a meta-mangerite from the Adirondack Complex, USA (Safonov, 1998).

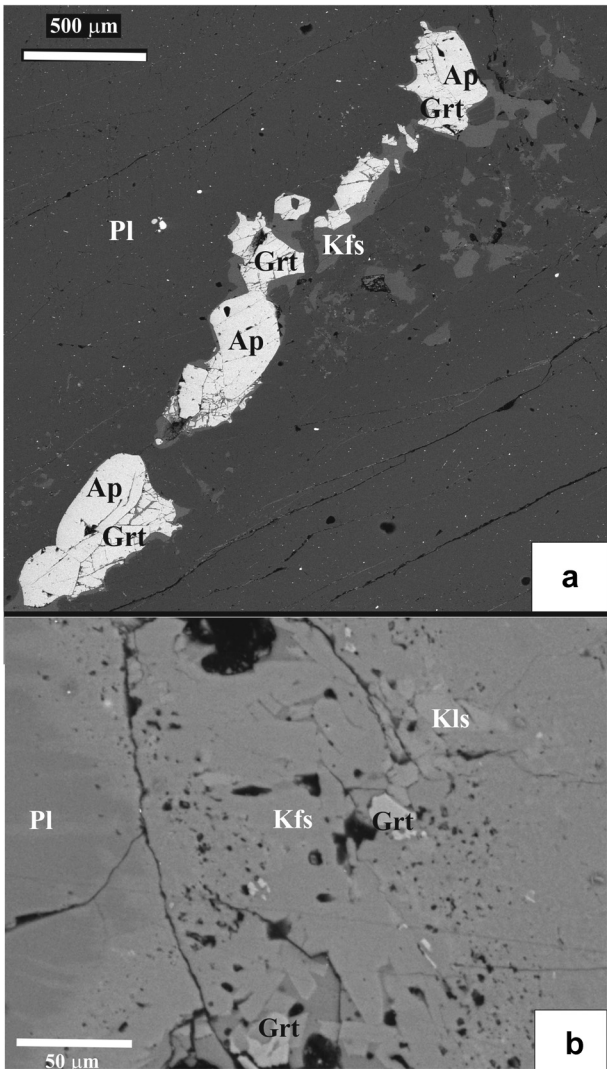

Figure 12. Grossular-rich garnet as an indicator of alkali activity. (a) Formation of grossular-rich garnet in an apatite-K-feldspar vein truncating plagioclase crystals in a meta-anorthosite from the Adirondack Complex, USA (Safonov, 1998). Formation of the vein is accompanied by K-feldspathization of the host plagioclase. The bright clustering of inclusions in plagioclase is magnetite; (b) formation of grossular-rich garnet in the assemblage with kalsilite due to strong K-feldspathization of plagioclase, which interacted with a H_2O-CO_2-KCl fluid at 800 °C and 550 MPa (Safonov et al., 2012).

procedure. For semi-quantitative calculations, it is not that necessary to know the specific alkali species in the fluids such that the thermodynamics of alkalis can be standardized to any species with well-constrained thermodynamic properties. For example, in order to demonstrate relations between charnockites and granites of southern India, Newton (1990) estimated the thermodynamic properties of several reactions between biotite, orthopyroxene, K-feldspar, plagioclase, quartz, and model liquids containing K and Na from a combination of the thermodynamic data from exchange reactions (1) and (8) in order to calculate diagrams in terms of temperature and log(K/Na) at constant pressure and H_2O activity. Perchuk et al. (1994) applied the thermodynamic properties of molten K_2CO_3 and Na_2CO_3 to the calculation of relations in charnockitic assemblages at constant T, P, and activities of H_2O and CO_2 in H_2O-CO_2 fluids in order to illustrate the transformation of biotite-quartz assemblage to orthopyroxene-K-feldspar for the Sulkava charnockites (southern Finland). Perchuk et al. (2000) applied the standard partial molar thermodynamic properties

and parameters of the equation of state for K^+, Na^+, and H^+ ions from the data base of Shock and Helgeson (1988) to compute phase relations in terms of $\log(K^+/H^+)$ and $\log(Na^+/H^+)$ for the system involving biotite-orthopyroxene-K-feldspar-plagioclase-quartz-fluid at constant P, T and a_{H_2O} in order to illustrate incipient charnockitization of tonalitic gneiss at Kurunegala (Sri Lanka). Safonov (1998) used a similar approach to calculate phase relations between orthopyroxene, clinopyroxene, garnet, plagioclase, K-feldspar and quartz in granulites from the Adirondack complex (USA).

In the present work we adopt a standard state for the alkalis as pure solid K_2O and Na_2O. Standard thermodynamic properties (enthalpy of formation from elements, entropy and volume) of the oxides at 298 K and 1 bar have been taken from the NIST database (http://webbook.nist.gov/cgi/cbook.cgi?Formula=k2o for K_2O and http://webbook.nist.gov/cgi/cbook.cgi?Formula=na2o for Na_2O). The heat capacity values reported in NIST have been converted to the polynomial recommended by Berman (1988) and Berman and Aranovich (1996). The calculations were performed using winTWQ (version 2.32) software (Berman, 2007) with the end-member mineral and solid solution properties according to Berman and Aranovich (1996) and Berman (2007). All calculations assumed the Gibbs free energy as a system potential.

To illustrate the validity of this approach, we have chosen three well-documented examples of incipient transformation of gneisses to charnockitic assemblages along local shear zones from South Africa, southern India, and Sri Lanka. These examples show clear changes in mineralogy from initial gneisses to newly formed charnockitic rocks, and thus allow a comparison of alkali activities employing various mineral reactions involved in one process.

Calculated relations between biotite, hornblende, orthopyroxene, plagioclase, K-feldspar, and quartz are shown on the $a_{K_2O} - T$ and $a_{H_2O} - a_{K_2O}$ diagrams (Fig. 13a and b). Compositions of coexisting minerals from a pyroxene-bearing dehydration zone in biotite-hornblende tonalitic gneisses (Bt + Hbl + Pl + Qtz) from the Causeway locality, Limpopo Complex, South Africa were used in the calculations (see Safonov et al., 2012; Rajesh et al., 2013 for textural relations and analytical data on the coexisting minerals). The dehydration zone is represented by a charno-enderbitic vein (Opx + Pl + Kfs + Qtz) across the gneiss. Safonov et al. (2012) deduced that the dehydration zone evolved within the temperature interval 650–800 °C and pressure 550–620 MPa under the influence of H_2O-CO_2-brines, which imposed a H_2O activity of around 0.2. Fig. 13a shows that at peak P-T, i.e. 800 °C and 620 MPa, transformation of the gneiss into charno-enderbite occurred via a decrease in the H_2O activity at a constant or slightly increasing a_{K_2O}. The gneiss initially did not contain K-feldspar. After dehydration, K-feldspar is present in small amounts as scattered exsolution lamellae in plagioclase or as K-feldspar micro-veins (Fig. 3a). Both hornblende and biotite in the gneiss are enriched in Al_2O_3 (up to 12 wt.% and up to 15 wt.%, respectively). It implies that the gneiss assemblage corresponds to a low a_{K_2O} in the rock. In order to quantify this value we calculated the equilibrium 7Ab + 14An + 16Phl + H_2O = 7Prg + 10Eas + 35Qtz + 3K_2O, which depends on a_{K_2O} much more than a_{H_2O}. Within the range $\log(a_{H_2O})$ from −1 to 0, this reaction indicates that $\log(a_{K_2O})$ ranges from −27.6 to −27.3 (see the inset in Fig. 13a). The transformation of the gneiss proceeds through the intermediate assemblage Bt + Opx + Pl + Qtz around the charno-enderbite vein, which is called the "transition zone" (Safonov et al., 2012; Rajesh et al., 2013). At fixed P-T, the K_2O activity in this assemblage can vary along the line defined by the equilibrium Al-Opx + 6En (Fs) + K_2O + 2H_2O = Phl (Ann) (where Al-Opx stands for the fictive Al_2O_3 end-member of the Opx solid solution) in the $\log(a_{H_2O}) - \log(a_{K_2O})$ diagram. This line has a gentle negative slope (Fig. 13a). For compositions of orthopyroxene and biotite from the transition zone (Rajesh et al., 2013), this equilibrium gives $\log(a_{K_2O})$ from −22.8 to −23.6 for the range of $\log(a_{H_2O})$ within the Bt + Opx + Pl + Qtz stability field (Fig. 13a). Appearance of the assemblage Opx + Kfs + Pl + Qtz is manifested by a lower H_2O activity, whereas the a_{K_2O} controls the Al content in Opx via the equilibrium Al-Opx + 6Qtz + K_2O = Kfs, which is an analogy of reaction (10). This equilibrium indicates a $\log(a_{K_2O})$ of about −23 at 620 MPa and 800 °C for the orthopyroxene composition from the charno-enderbite vein (Fig. 3a, b). This value is comparable to the $\log(a_{K_2O})$ calculated for the transition zone. Thus, the difference in mineralogy between the transition zone and the charno-enderbite vein is mainly caused by variations in the H_2O activity within the dehydration domain for a nearly constant a_{K_2O}. Nevertheless, the $\log(a_{K_2O})$ values for the transition zone and the charnockite vein are much higher than those for the surrounding biotite-hornblende gneiss suggesting that the formation of the dehydration domain was governed by both increase of the alkali activity and decrease of the H_2O activity in fluids.

Further evolution of the charno-enderbite vein, during cooling to 650–700 °C, was accompanied by the formation of new pargasite-edenite amphibole and biotite after orthopyroxene (Safonov et al., 2012), as well as the formation of K-feldspar micro-veins between plagioclase and quartz grains, which have been interpreted as indicators of an increase in the alkali activity (Safonov et al., 2012; Rajesh et al., 2013). In fact, Fig. 13a and b shows that the assemblages Hbl + Opx + Pl + Kfs and Hbl + Bt + Opx + Kfs form after the assemblage Opx + Pl + Kfs + Qtz via an increase in a_{K_2O} ($\log(a_{K_2O}) > -22$) during cooling. In addition, Safonov et al. (2012) documented the presence of clinopyroxene-orthopyroxene-K-feldspar reaction textures replacing biotite (Fig. 6) in the surrounding amphibole-biotite gneiss and interpreted those textures as a result of reaction (4), which occurred during cooling at temperatures below 700 °C. The positive slope of this reaction in the diagram (Fig. 13b) supports this conclusion. However, the alkali activity sensor for this process is reaction (14) between coexisting pyroxenes, K-feldspar, plagioclase and quartz, which does not depend on the H_2O activity (Fig. 13b). The inset in Fig. 13b shows the calculated position of this equilibrium. At a temperature of 670 °C (the average temperature for the formation of the pyroxene-K-feldspar coronas; Safonov et al., 2012), it corresponds to a $\log(a_{K_2O}) = -25.7$. Estimates based on the reaction Al-Opx + 6Qtz + K_2O = Kfs give a close value of $\log(a_{K_2O}) = -25.8$. These values are slightly lower than the $\log(a_{K_2O})$ for the charno-enderbite vein and the transition zone because of the lower temperature. Nevertheless, they are significantly higher than those estimated for the gneiss at 800 °C. This fact supports the conclusion by Safonov et al. (2012) that the leading factor for the origin of the pyroxene-K-feldspar coronas in the gneiss at relatively low temperature was the high K activity in the late stage fluids acting within the dehydration domain.

Transformation of biotite-hornblende gneisses to charnockites is a widespread phenomenon in the Precambrian complexes of Southern India and Sri Lanka, where this process has been called "incipient" or "arrested" charnockitization (Janardhan et al., 1982; Hansen et al., 1984, 1987; Stähle et al., 1987; Burton and O'Nions, 1990; Perchuk et al., 2000; Ravindra Kumar, 2004). Perchuk et al. (2000) suggested that along with the decrease in H_2O activity caused by infiltrating CO_2-bearing fluids (e.g. Hansen et al., 1987), the transformation was provoked by an elevated alkali activity in these fluids at temperatures up to 740 °C and at about 600 MPa. To confirm this suggestion, Perchuk et al. (2000) considered the alumina-zoning pattern in orthopyroxene grains surrounded by the K-feldspar micro-veins in the charnockite from Kurunegala, Sri Lanka. They ascribed the observed regular decrease in Al to the operation of reaction (10). In order to check this conclusion, we

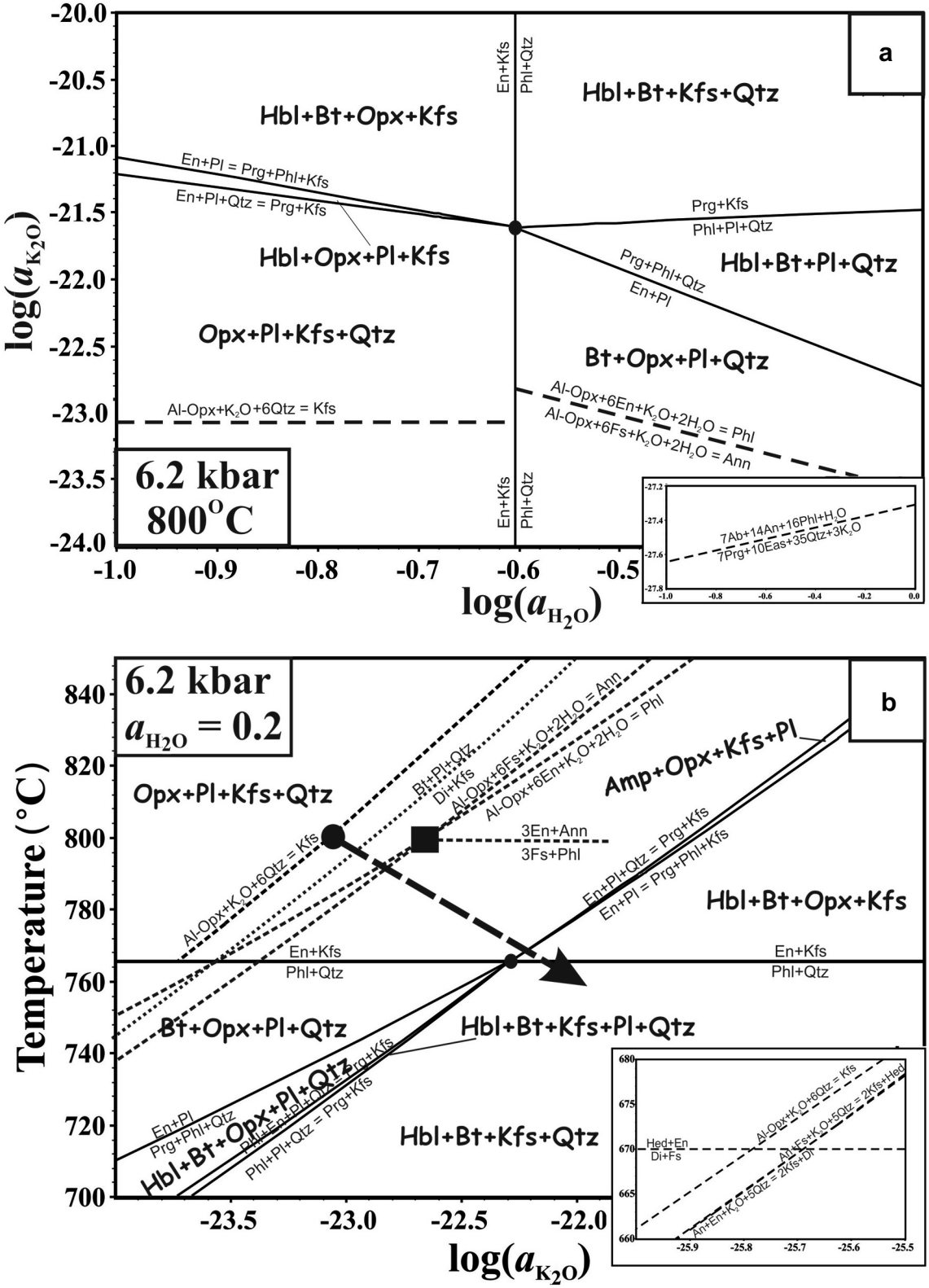

Figure 13. Diagrams illustrating variations in a_{K_2O} as a function of temperature and H_2O activity during the transformation of a tonalitic biotite-hornblende gneiss to charno-enderbite at the Causeway locality, Limpopo Complex, South Africa (Safonov et al., 2012; Rajesh et al., 2013). (a) Diagram of $\log(a_{K_2O}) - \log(a_{H_2O})$ at 620 MPa and 800 °C demonstrating the relative stability of various mineral assemblages and the position of equilibria as a function of K_2O activity in these assemblages: Al-Opx + 6Qtz + K_2O = Kfs for Opx + Kfs + Pl + Qtz and Al-Opx + 6En (Fs) + K_2O + $2H_2O$ = Phl (Ann) for Opx + Bt + Pl + Qtz. The inset shows the position of the equilibrium 7Ab + 14An + 16Phl + H_2O = 7Prg +10Eas + 35Qtz + $3K_2O$, which determines the K_2O activity in the host gneiss; (b) diagram $\log(a_{K_2O}) - T$ at 620 MPa and a_{H_2O} = 0.2 demonstrating the relative stability of various mineral assemblages and the position of equilibria, which determine the K_2O activity and temperature in these assemblages: Al-Opx + 6Qtz + K_2O = Kfs for Opx + Kfs + Pl + Qtz (black dot) and Al-Opx + 6En (Fs) + K_2O + $2H_2O$ = Phl (Ann) for Opx + Bt + Pl + Qtz (black square). The dotted line indicates the position of reaction (4), which results in the local formation of clinopyroxene-K-feldspar assemblages in the gneiss. The inset shows the position of the equilibrium An + 16En (Fs) + K_2O + 5Qtz = 2Kfs + Di (Hed), which determines the K_2O activity for the two pyroxene-K-feldspar assemblage in the gneiss. Dashed arrow shows the arbitrary path of evolution for mineral assemblages in the charno-enderbite vein on cooling.

used mineral analyses from the gneiss and charnockite to compare a_{K_2O} for these assemblages. In contrast to the biotite-hornblende gneiss from the Causeway locality described above, the gneiss at Kurunegala initially contained K-feldspar, while hornblende and biotite in the rock are poorer in Al_2O_3 (about 10 wt.% and 13 wt.%, respectively). This suggests that the gneiss at Kurunegala should buffer higher a_{K_2O}. The equilibrium 4Phl + 3Ab + 6An + 15Qtz + $3K_2O$ = 3Prg + 10Kfs + H_2O relevant for the gneiss returns a $\log(a_{K_2O})$ from −22.6 to −22.9 at 740 °C and 600 MPa for the $\log(a_{H_2O}) = -1$ to 0 (Fig. 14). In fact, these values are much higher than the $\log(a_{K_2O})$ for the K-feldspar-free gneiss from the Causeway locality. The Opx + Bt + Kfs + Qtz assemblage, inside the charnockite patch, allows for the calculation of $\log(a_{K_2O}) = -23.8$ at $\log(a_{H_2O}) = -0.55$ for 740 °C and 600 MPa (Fig. 14). Perchuk et al. (2000) noticed the presence of rare clinopyroxene at the grain boundaries between orthopyroxene and plagioclase in the leucocratic plagioclase-K-feldspar-quartz zone (KPQ zone in Perchuk et al., 2000) at the periphery of the charnockite patch. The H_2O-independent reactions En + An + 5Qtz + K_2O = Di + 2Kfs, Al-Opx + 6Qtz + K_2O = Kfs and 6En + 6An = 6Di + 5Al-Opx + 2Kfs give a $\log(a_{K_2O})$ of about −24.0, which is very close to the value for the charnockite (Fig. 14).

Along with the biotite-hornblende gneisses, incipient charnockitization in Southern India and Sri Lanka is also developed after K-feldspar-bearing biotite-garnet gneisses (leptinites) (Srikantappa et al., 1985; Ravindra Kumar et al., 1985; Hansen et al., 1987; Raith and Srikantappa, 1993; Rajesh et al., 2011). Fig. 15a and b illustrates an example of the transformation of leptinite to charnockite at Ponmudi, Kerala, southern India (e.g. Hansen et al., 1987). The process is manifested by a notable decrease in the amount of biotite and garnet and an increase in alkali feldspar in the charnockites relative to the host gneiss. This indicates consummation of both biotite and garnet during the orthopyroxene-forming reaction. Although garnet is preserved in charnockite, Raith and Srikantappa (1993) and Rajesh et al. (2011) described its corrosion by orthopyroxene, plagioclase and K-feldspar. The modal abundance of plagioclase is not markedly different suggesting that this phase is passive in the process. Raith and Srikantappa (1993) noticed that the charnockite was separated from the host gneiss by a garnet-bearing transition zone with a low modal amount of biotite. According to the above studies, the physical parameters for the incipient charnockitization correspond to 700 to 800 °C, 500–550 MPa, and a H_2O activity close to 0.2 (e.g. Hansen et al., 1987). Garnet-biotite and garnet-orthopyroxene thermometry applied to the gneiss and the charnockite mineral pairs from the Ponmudi locality (sample 147–214 from the paper by Hansen et al., 1987) gives close temperature estimates of 770 and 790 °C, respectively at 500 MPa (Fig. 15b), thus confirming the nearly isothermal character of the transformation. The $\log(a_{K_2O})$ values calculated within this temperature range (−23.7 for the charnockite and −24.5 for the gneiss; Fig. 15b), are very close to each other. There the difference is mostly related to the difference in temperature estimates using garnet-biotite and garnet-orthopyroxene Fe-Mg exchange reactions. The $\log(a_{K_2O})$ estimates calculated for the charnockite from the H_2O-independent reactions Prp(Alm) + 6Qtz + K_2O = 2Kfs + 3En(Fs) and Al-Opx + 6Qtz + K_2O = Kfs fall well within the field Grt + Opx + Kfs (Fig. 15a, b). However, the $\log(a_{K_2O})$ estimates for the gneiss at $a_{H_2O} = 0.2$ (Fig. 15b) are not located in the fields of the gneiss assemblages Grt + Bt + Qtz and Grt + Bt + Kfs. The boundaries of these fields greatly expand to both higher temperature and $\log(a_{K_2O})$ with increasing a_{H_2O}. Already at $a_{H_2O} = 0.4$ the $\log(a_{K_2O})$

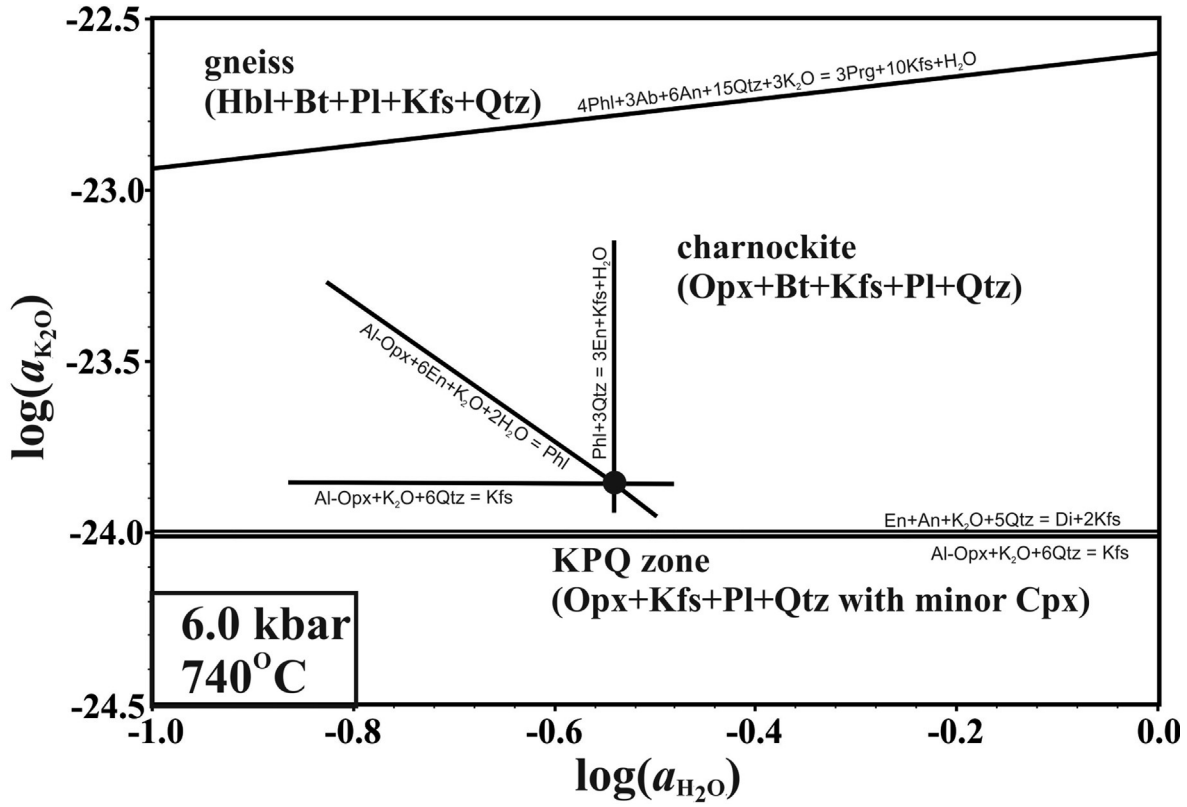

Figure 14. Diagram $\log(a_{K_2O}) - \log(a_{H_2O})$ at 600 MPa and 740 °C showing K_2O activities in fluids coexisting with the charnockite core and leucocratic KPQ zone from the charnockite patch in comparison to the host K-feldspar-bearing hornblende-biotite gneiss at Kurunegala, Sri Lanka (Perchuk et al., 2000).

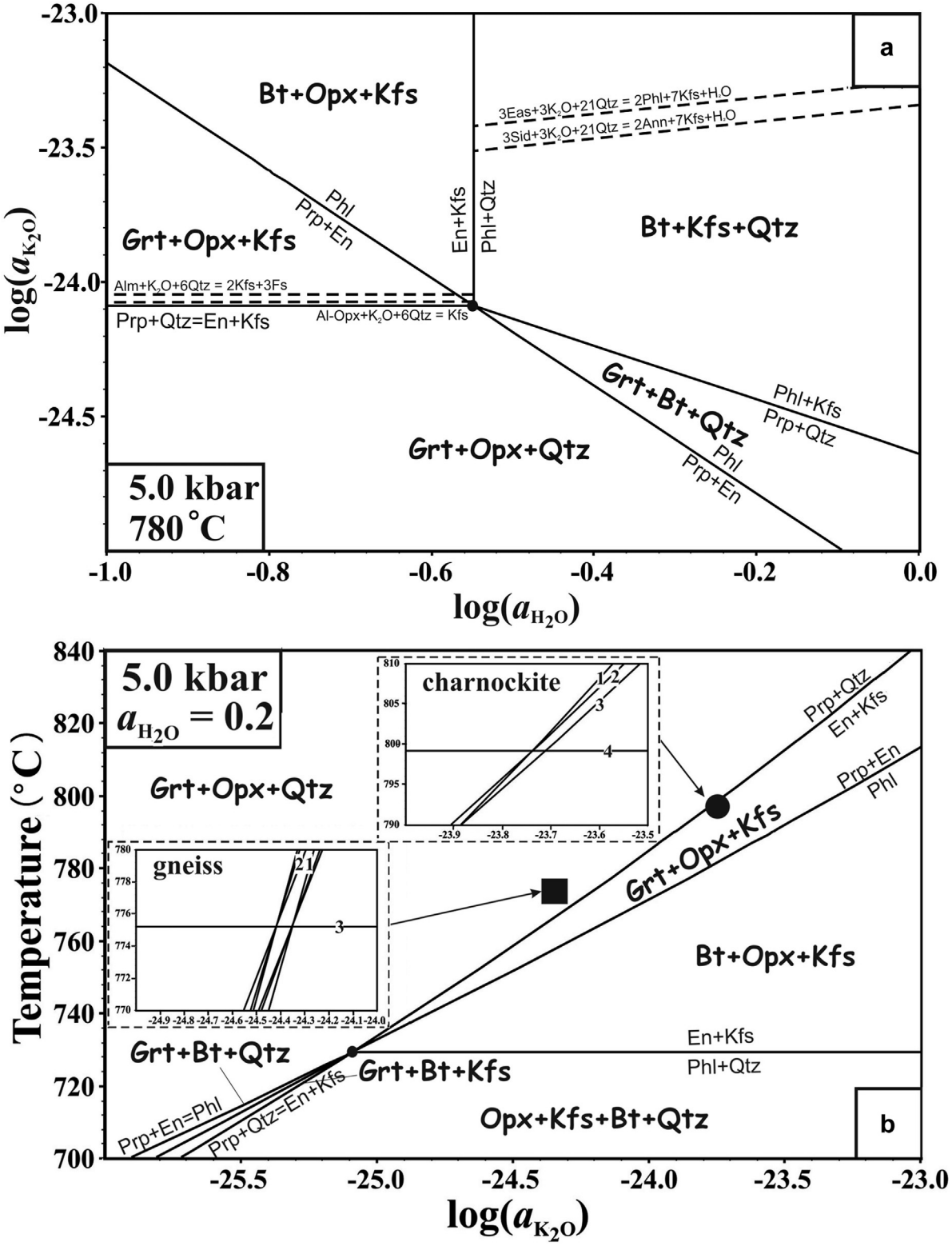

Figure 15. Diagrams illustrating variations in a_{K_2O} as a function of temperature and H_2O activity during the transformation of a garnet-biotite-K-feldspar gneiss to a garnet-bearing charnockite at Ponmudi, Kerala, southern India (Hansen et al., 1987). (a) Diagram $\log(a_{K_2O}) - \log(a_{H_2O})$ at 500 MPa and 780 °C demonstrating the relative stability of various mineral assemblages and the positions of equilibria, which determine the K_2O activity in these assemblages: Al-Opx + 6Qtz + K_2O = Kfs and Prp(Alm) + 6Qtz + K_2O = 3En (Fs) + 2Kfs for Grt + Opx + Kfs and 3Eas (Sid) + 3K_2O + 21Qtz = 2Phl (Ann) + 7Kfs + H_2O for Bt + Kfs + Qtz; (b) diagram $\log(a_{K_2O}) - T$ at 500 MPa and a_{H_2O} = 0.2 demonstrating the relative stability of various mineral assemblages. The insets show the positions of the equilibria determining the K_2O activity and temperature for the charnockite (black dot) and gneiss (black square). The numbers in the charnockite inset: (1) Prp + 6Qtz + K_2O = 3En + 2Kfs, (2) Alm + 6Qtz + K_2O = Fs + 2Kfs, (3) Al-Opx + 6Qtz + K_2O = Kfs, (4) Prp + 3Fs = Alm + 3En. The numbers in the gneiss inset: (1) 7Alm + 8H_2O + 4 K_2O = 3Sid + 5Ann, (2) 7Prp + 8H_2O + 4 K_2O = 3Eas + 5Phl, (3) Prp + Ann = Alm + Phl.

estimates fall into these fields. Thus, the transformation of garnet-biotite-K-feldspar gneiss (leptinite) to garnet-bearing charnockite at Ponmudi (Hansen et al., 1987) was governed by decrease of the H_2O activity leading to biotite breakdown, but seems to be unrelated to variations in alkali activity.

4. Discussion

The present calculations demonstrate different regimes of alkali activity during specific metamorphic processes. The K_2O activity in fluids that equilibrated with the host gneisses at Kurunegala and Ponmudi are somewhat higher than those that equilibrated with the charnockites (Figs. 14 and 15). This result is in contrast with examples from the Causeway locality where the K_2O activity, estimated for the gneiss, is significantly lower than that for the charnockite (Fig. 13). At all three localities, transformation of gneisses occurred along local shear zones under similar P-T conditions, and was caused by the infiltration of CO_2 and brine fluids, traces of which are preserved in fluid inclusions (Perchuk et al., 2000; Rajesh et al., 2013). The contrast in alkali behavior between Kurunegala and Ponmudi on the one hand, and Causeway on the other, is most likely related to the differences in the original mineralogy of the gneisses, the namely, absence of K-feldspar in the Causeway gneisses and the abundance of this mineral in the Kurunegala and Ponmudi gneisses. The alkali activities in H_2O-CO_2-salt fluids invading the Kurunegala gneisses along the shear zones were buffered by the plagioclase-K-feldspar-quartz assemblage via equilibria (1)–(3). A similar situation seems to be valid for the Ponmudi, as well. The fluids entering the Causeway gneisses were unbuffered because of the absence of K-feldspar in the rocks. The unbuffered alkalis regime in the Causeway rocks is texturally manifested by the abundant K-feldspar micro-veins developed along the plagioclase grain boundaries with quartz, hornblende and biotite. These reaction textures are absent in the Kurunegala and Ponmudi gneisses, where the lowering of the H_2O activity (Hansen et al., 1987; Stähle et al., 1987; Burton and O'Nions, 1990; Perchuk et al., 2000) was probably the major factor for the incipient charnockitization.

Our calculations indicate that variations in alkali activity alone cannot result in the development of totally anhydrous assemblages after biotite and/or amphibole-bearing gneisses. Moreover, increasing the K_2O activity stabilizes biotite and amphibole towards higher temperature (Figs. 13b, 14 and 15b) or lower H_2O activity (Figs. 13a, 14 and 15a). The resulting mineral assemblage is strongly dependent on the ratio of H_2O and alkali activities. A concomitant lowering of the H_2O activity is required for the complete dehydration as indicated by numerous petrological and theoretical studies (Hansen et al., 1995; Newton, 1995; Franz and Harlov, 1998; Harlov et al., 1998; Newton et al., 1998; Harlov and Wirth, 2000; Perchuk et al., 2000; Harlov and Förster, 2002; Montanini and Harlov, 2006; Newton and Manning, 2010; Touret and Huizenga, 2011; Rajesh et al., 2013; Touret and Nijland, 2013). According to the experimental data, the most plausible medium providing a simultaneous increase in the alkali activity and decrease in the H_2O activity appears to be complex aqueous solutions of strong electrolytes with a certain amount of dissolved non-electrolytes (primarily, CO_2) (Aranovich et al., 1987, 2013; Aranovich and Newton, 1996, 1997; Shmulovich and Graham, 1996). Fluid inclusion studies in high-grade rocks (see recent reviews in Touret and Huizenga, 2011; Touret and Nijland, 2013) have shown that the most abundant strong electrolyte solute in high-grade fluids is (Na, K)Cl, with subordinate alkali carbonates and alkali earth chlorides. Strong ionization of the (K, Na)Cl-H_2O solutions at pressures above 300–400 MPa and temperatures 600–900 °C results in a decrease in the H_2O activity in these fluids, which becomes approximately proportional to $X^2_{H_2O}$ (Aranovich and Newton, 1996, 1997; Aranovich et al., 2010). The ratio of H_2O and alkali activities in the chloride-bearing fluids is a complex function of temperature, pressure, bulk chloride content and concentrations of additional components. The alkali chloride activities in the aqueous-salt fluids decrease with increasing pressure, but not as drastically as the activity of H_2O (Aranovich and Newton, 1996, 1997). Equations of Aranovich and Newton (1996, 1997) for the H_2O-NaCl and H_2O-KCl fluids indicate that the activity of alkali chlorides in these fluid increases non-linearly with the decrease of H_2O activity. In addition, according to the equations suggested for the H_2O-CO_2-NaCl ternary fluid (Aranovich et al., 2010), the increase of the CO_2 content in the fluid should lead to an increase in the alkali activity at similar H_2O activity values. This effect should be even stronger for the immiscible aqueous-salt and CO_2-rich fluids.

Mineral assemblages corresponding to various alkali activities should reflect different fluid compositions. The assemblages clinopyroxene + K-feldspar, K-rich hornblende + K-feldspar, grossular-rich garnet + K-feldspar, formed under a high alkali/water activity ratio, are indicative of highly saline fluids likely to coexist with the CO_2-rich fluid. This hypothesis can be evaluated by the Cl-contents of hornblende or accessory apatite, as it was shown above for mangerites and anorthosites from the Adirondack Complex and the amphibolite from the Southern Marginal Zone of the Limpopo Complex (Figs. 9a, b, 11 and 12a). It is also supported by the results of experimental studies (Safonov et al., 2012). Such fluids produce spectacular local-scale reaction textures in the rocks. In contrast, charnockitic assemblages can be considered as indicators of aqueous-carbonic fluids with relatively low alkali activities.

The approach for calculating alkali activities proposed in this paper appears to be more general compared to those suggested by Newton (1990) and Perchuk et al. (1994, 2000), since it allows for quantitative estimates and comparisons of the alkali activity in various assemblages, even in the absence of detailed information on the fluid composition in terms of the major volatile components except H_2O. If needed, activities or chemical potentials of (virtual) alkali oxides, retrieved from the calculations, can be converted into the activities of realistic alkali-bearing species in the fluid phase provided that some additional information on the major fluid composition is available for the assemblage under consideration. For example, if the CO_2 activity in the fluid phase can be independently estimated from a phase assemblage, the Na_2CO_3 activity in the fluid phase may be retrieved from the equilibrium constant for the reaction $Na_2O + CO_2 = Na_2CO_3$. Similarly, the HCl fugacity in the fluid can be estimated independently from the Cl content in biotite, amphibole, and/or apatite (Zhu and Sverjensky, 1991). The (virtual) activity of Na_2O in a rock can be converted into the NaCl activity in the fluid phase by considering the equilibrium $Na_2O + 2HCl = 2NaCl + H_2O$. Similar reactions can be applied for the recalculation of the K_2O activity into the activity of the K-bearing fluid species.

Very low calculated values of the virtual K_2O activity in the rocks do not imply low concentrations of K-species in the equilibrium fluid. For example, if the HCl/H_2O activity ratio in the fluid is around 10^{-4} and $a(H_2O)$ is around 0.5 corresponding to $X_{Cl} = Cl/(Cl + OH) = 0.02$ in the biotite with $X_{Mg} = 0.5$ (Zhu and Sverjensky, 1992), for a rock with $a(K_2O) = 10^{-22}$ the KCl activity in the fluid would be close to 0.1 at 700 °C and 500 MPa.

In general, a similar approach for activity calculation can be applied for other components. For example, reaction (3) shows the dependence of the feldspar equilibrium on the CaO activity. Reactions (4) and (15), which describe the formation of the assemblage clinopyroxene + K-feldspar after biotite + plagioclase + quartz or orthopyroxene + plagioclase + quartz, can be rewritten as being controlled by the CaO activity and, thus, can serve as tools for estimation of its activity.

In calculating the diagrams in Figs. 13–15, we assumed the Gibbs free energy as a system potential. If the process is metasomatic *senso stricto,* i.e. proceeding at constant volume (e.g. Putnis and Austrheim, 2013), the Helmholtz free energy should be used instead. That would lead to significantly different phase diagrams (Connolly, 2009). Developing an approach that would utilize the Helmholtz free energy for phase diagram calculations is a problem left to future research.

5. Conclusions

(1) Certain assemblages in high-grade rocks provide clear examples of mineral reactions controlled by K and/or Na activities in the fluids, which should be considered as additional intensive parameters for metamorphic systems;

(2) The suggested semi-quantitative thermodynamic approach based on the calculation of virtual K_2O and Na_2O activities allows for comparison of these parameters for the rocks affected by fluids. The calculations for three specific examples of rock-fluid interaction from South Africa, southern India and Sri Lanka have revealed two contrasting regimes for alkali activities. These include the rock-buffered and the unbuffered, which are determined by the original mineral assemblage present in rocks interacting with fluids. The rock-buffered regime means that when passing through rocks composed of the appropriate mineral assemblage, alkali activities in the fluids can be easily adjusted to the activities of these components in the rocks. In this case, alkali activities are not leading factors of rock transformation. In contrast, for the unbuffered regime alkali activities are the determining factors during fluid-rock interaction along with the activities of other fluid species;

(3) Although various rocks can be formally compared with each other in terms of their alkali oxide potential (activity) values, only when clear macroscopic and/or microscopic textural evidence for the variability of alkali activities, such as reaction textures or regional or local-scale transformation of rock (dehydration zones, metasomatic contact aureoles, etc.) can be demonstrated, the alkali activity diagrams of the type proposed here (Figs. 13–15) may apply. The necessary preposition for the calculation of alkali or other oxide activities is the suggestion that a fluid really existed in the system. The alkali oxides activity values that can be estimated from the appropriate phase assemblages are by no means directly related to the amount of alkalis present in the rocks. Rocks composed of the same mineral assemblage, having the same composition of minerals but differing in bulk proportion of minerals would, nevertheless, have the same alkali activity. That is what differs the perfectly mobile components from the inert ones in the sense of Korzhinskii (1959) and Thompson (1959).

Acknowledgments

Authors thank Rob Berman (Natural Resources Canada) for recalculating the NIST heat capacity values into the Berman (1988) format. Helpful comments by Ted Labotka and anonymous reviewer improved the manuscript. Daniel Harlov is thanked for his editorial supervision and correction of the manuscript. The study was supported by Russian Foundation for Basic Research (projects 13-05-00353a to OGS, 12-05-00303a to LYA), Federal Task Program 3586, and by grants from the National Science Foundation of South Africa (GUN: 2053192) and University of Johannesburg as part of the Russian-South African scientific collaboration.

References

Aranovich, L.Ya, Newton, R.C., 1996. H_2O activity in concentrated NaCl solutions at high pressures and temperatures measured by the brucite-periclase equilibrium. Contributions to Mineralogy and Petrology 125, 200–212.

Aranovich, L.Ya, Newton, R.C., 1997. H_2O activity in concentrated KCl and KCl-NaCl solutions at high temperatures and pressures measured by the brucite-periclase equilibrium. Contributions to Mineralogy and Petrology 127, 261–271.

Aranovich, L. Ya., Shmulovich, K.I., Fed'kin, V.V., 1987. The H_2O and CO_2 regime in regional metamorphism. International Geology Review 29, 1379–1401.

Aranovich, L.Y., Zakirov, I.V., Sretenskaya, N.G., Gerya, T.V., 2010. Ternary system H_2O-CO_2-NaCl at high P-T parameters: an empirical mixing model. Geochemistry International 48, 446–455.

Aranovich, L.Y., Newton, R.C., Manning, C.E., 2013. Brine-assisted anatexis: experimental melting in the system haplogranite-H_2O-NaCl-KCl at deep-crustal conditions. Earth and Planetary Science Letters 374, 111–120.

Berman, R.G., 1988. Internally-consistent thermodynamic data for stoichiometric minerals in the system Na_2O-K_2O-CaO-MgO-FeO-Fe_2O_3-Al_2O_3-SiO_2-TiO_2-H_2O-CO_2. Journal of Petrology 29, 445–522.

Berman, R.G., 2007. WinTWQ (version 2.3): a software package for performing internally-consistent thermobarometric calculations. Geological Survey of Canada Open File 5462.

Berman, R.G., Aranovich, L.Ya, 1996. Optimized standard state and solution properties of minerals I model calibration for olivine, orthopyroxene, cordierite, garnet, and ilmenite in the system FeO-MgO-CaO-Al_2O_3-TiO_2-SiO_2. Contributions to Mineralogy and Petrology 126, 1–24.

Burton, K.W., O'Nions, R.K., 1990. The timescale and mechanism of granulite formation at Kurunegala, Sri Lanka. Contributions to Mineralogy and Petrology 106, 66–89.

Connolly, J.A.D., 2009. The geodynamic equation of state: what and how. Geochemistry, Geophysics, Geosystems 10, Q10014.

Eskola, P., 1956. Postmagmatic potash metasomatism of granite. Bulletin de la Commission géologique de Finlande 172, 85–100.

Franz, L., Harlov, D.E., 1998. High-grade K-feldspar veining in granulites from the Ivrea-Verbano Zone, Northern Italy: fluid flow in the lower crust and implications for granulite facies genesis. Journal of Geology 106, 455–472.

Hansen, E.C., Harlov, D.E., 2007. Whole-rock, phosphate, and silicate compositional trends across an amphibolite- to granulite-facies transition, Tamil Nadu, India. Journal of Petrology 48, 1641–1680.

Hansen, E.C., Newton, R.C., Janardhan, A.S., 1984. Fluid inclusions in rocks from amphibolite facies gneiss to charnockite progression in southern Karnataka, India: direct evidence concerning the fluids of granulite metamorphism. Journal of Metamorphic Geology 2, 249–264.

Hansen, E.C., Janardhan, A.S., Newton, R.C., Prame, W.K.B.N., Kumar, G.R.R., 1987. Arrested charnockite formation in South India and Sri Lanka. Contributions to Mineralogy and Petrology 97, 225–244.

Hansen, E.C., Newton, R.C., Janardhan, A.S., Lindberg, S., 1995. Differentiation of Late Archean crust in the Eastern Dharwar craton, South India. Journal of Geology 103, 629–651.

Harlov, D.E., 2004. Fluid Induced Dehydration of Mafic Lower Crust from Amphibolite to Granulite Facies: Nature and Experiment. American Geophysical Union, Fall Meeting, V31A-1409.

Harlov, D.E., 2012. The potential role of fluids during regional granulite facies dehydration in the lower crust. Geoscience Frontiers 3, 813–827.

Harlov, D.E., Förster, H.-J., 2002. High-grade fluid metasomatism on both a local and regional scale: the Seward Peninsula, Alaska and the Val Strona di Omegna, Ivrea–Verbano Zone, northern Italy. Part I: petrography and silicate mineral chemistry. Journal of Petrology 43, 769–799.

Harlov, D.E., Hansen, E.C., Bigler, C., 1998. Petrologic evidence for K-feldspar metasomatism in granulite facies rocks. Chemical Geology 151, 373–386.

Harlov, D.E., Johansson, L., Van den Kerkhof, A., Förster, H.J., 2006. The role of advective fluid flow and diffusion during localized, solid-state dehydration: Söndrum Stenhuggeriet, Halmstad, SW Sweden. Journal of Petrology 47, 3–33.

Harlov, D.E., Wirth, R., 2000. K-feldspar-quartz and K-feldspar-plagioclase phase boundary interactions in garnet-orthopyroxene gneisses from the Val Strona di Omegna, Ivrea Verbano Zone, northern Italy. Contributions to Mineralogy and Petrology 140, 148–162.

Iiyama, J.T., 1965. Influence des anions sur les équilibres d'échange dions Na-K dans les feldspaths alcalins a 600 °C sous une pression de 1000 bars. Bulletin de la Societé francaise de Minéralogie et de Cristallographie 88, 618–622.

Janardhan, A.S., Newton, R.C., Hansen, E.C., 1982. The transformation of amphibolite facies gneiss to charnockite in Southern Karnataka and Northern Tamil Nadu, India. Contributions to Mineralogy and Petrology 79, 130–149.

Knudsen, T.L., Lidwin, A., 1996. Magmatic CO_2, brine and nitrogen inclusions in Sveconorwegian enderbitic dehydration veins and a gabbro from the Bamble sector, southern Norway. European Journal of Mineralogy 8, 1041–1064.

Korikovsky, S.P., Kislyakova, N.G., 1975. Reaction textures and phase relations in hypersthene-sillimanite crystalline schists of the Sutam Complex of the Aldan Shield. In: Metasomatism and ore formation (Metasomatity i orudenenie). Nauka, Moscow, pp. 314–342.

Korikovsky, S.P., Aranovich, L.Y., 2010. Charnockitization and enderbitization of mafic granulites in the Porya Bay Area, Lapland Granulite Belt, Southern Kola Peninsula: I. petrology and geothermobarometry. Petrology 18, 320–349.

Korzhinskii, D. S., 1946. Principles of alkali mobility during magmatic phenomena. Proceedings dedicated to Acad.. D.S. Belyankin, Izdatel'stvo AN SSSR (in Russian).
Korzhinskii, D.S., 1959. Physical-chemical Basis of the Analysis of the Parageneses of Minerals (English Translation). Consultants Bureau Inc., New York.
Korzhinskii, D.S., 1962. The role of alkalinity in the formation of charnockitic gneisses. Trudy Vostochno-Sibirskogo Instituta Academii Nauk SSSR Series of Geology 5, 50–61 (in Russian).
Labotka, T.C., Cole, D.R., Fayek, M., Riciputi, L.R., Stadermann, F.J., 2004. Coupled cation and oxygen-isotope exchange between alkali feldspar and aqueous chloride solution. American Mineralogist 89, 1822–1825.
Larikova, T.L., Zaraisky, G.P., 2009. Experimental modeling of corona textures. Journal of Metamorphic Geology 27, 139–151.
Montanini, A., Harlov, D.E., 2006. Petrology and mineralogy of granulite-facies mafic xenoliths (Sardinia, Italy): evidence for KCl metasomatism in the lower crust. Lithos 92, 588–608.
Newton, R.C., 1990. Fluids and melting in the Archean deep crust of Southern India. In: Ashworth, J.R., Brown, M. (Eds.), High-Temperature Metamorphism and Crustal Anatexis, The Mineralogical Society Series 2, London, Unwin Human, pp. 149–179.
Newton, R.C., 1995. Simple-system mineral reactions and high-grade metamorphic fluids. European Journal of Mineralogy 7, 861–881.
Newton, R.C., Manning, C.A., 2010. Role of saline fluids in deep-crustal and upper-mantle metasomatism: insights from experimental studies. Geofluids 10, 58–72.
Newton, R.C., Aranovich, L.Y., Hansen, E.C., Vandenheuvel, B.A., 1998. Hypersaline fluids in Precambrian deep-crustal metamorphism. Precambrian Research 91, 41–63.
Norberg, N., Neusser, G., Wirth, R., Harlov, D., 2011. Microstructural evolution during experimental albitization of K-rich alkali feldspar. Contributions to Mineralogy and Petrology 162, 531–546.
Norberg, N., Harlov, D.E., Neusser, G., Wirth, R., Rhede, D., Morales, L., 2013. Experimental development of patch perthite from synthetic cryptoperthite: microstructural evolution and chemical re-equilibration. American Mineralogist 98, 1429–1441.
Orville, P.M., 1962. Alkali metasomatism and feldspars. Norsk Geologisk Tidsskrift 42, 283–316.
Orville, P.M., 1963. Alkali ion exchange between vapor and feldspar phases. American Journal of Science 261, 201–237.
Parfenova, O.V., Guseva, E.V., 2000. Feldspars of enderbite-charnockite complexes indicators of alkalinity during charnockitization of schists. Geochemistry International 38, 856–866.
Perchuk, L.L., Gerya, T.V., 1992. The fluid regime of metamorphism and the charnockite reaction in granulites: a review. International Geology Review 34, 1–58.
Perchuk, L.L., Gerya, T.V., 1993. Fluid control of charnockitization. Chemical Geology 108, 175–186.
Perchuk, L.L., Gerya, T.V., Korsman, K., 1994. A model for charnockitization of gneissic complexes. Petrology 2, 451–479.
Perchuk, L.L., Safonov, O.G., Gerya, T.V., Fu, B., Harlov, D.E., 2000. Mobility of components in metasomatic transformation and partial melting of gneisses: an example from Sri-Lanka. Contributions to Mineralogy and Petrology 140, 212–232.
Putnis, A., Austrheim, H., 2013. Mechanism of metasomatism and metamorphism on the local mineral scale: the role of dissolution-precipitation during mineral re-equilibration. In: Harlov, D.E., Austrheim, H. (Eds.), Metasomatism and the Chemical Transformation of Rock. The Role of Fluids in Terrestrial and Extraterrestrial Processes. Springer, pp. 141–170.
Putnis, A., Hinrichs, R., Putnis, C.V., Golla-Schindler, U., Collins, L.G., 2007. Hematite in porous red-clouded feldspars: evidence of large-scale crustal fluid–rock interaction. Lithos 95, 10–18.
Raith, M., Srikantappa, C., 1993. Arrested charnockite formation at Kottavattam, southern India. Journal of Metamorphic Geology 11, 815–832.
Rajesh, H.M., Belyanin, G.A., Safonov, O.G., Kovaleva, E.I., Golunova, M.A., van Reenen, D.D., 2013. Fluid-induced dehydration of the paleoarchean Sand River biotite-hornblende gneiss, Central Zone, Limpopo Complex, South Africa. Journal of Petrology 54, 41–74.
Rajesh, H.M., Santosh, M., Yoshikura, S., 2011. The Nagercoilcharnockite: a magnesian, calcic to calc-alkalicgranitoid dehydrated during a granulite-facies metamorphic event. Journal of Petrology 52, 375–400.
Ravindra Kumar, G.R., 2004. Mechanism of arrested charnockite formation at Nemmara, Palghat region, southern India. Lithos 75, 331–358.
Ravindra Kumar, G.R., Srikantappa, C., Hansen, E.C., 1985. Charnockiteformation at Ponmudi, southern India. Nature 313, 207–209.
Safonov, O.G., 1998. The role of alkalis in the formation of coronitic textures in metamangerites and metaanorthosites from the Adirondack Complex, United States. Petrology 6, 583–602.
Safonov, O.G., Kovaleva, E.I., Kosova, S.A., Rajesh, H.M., Belyanin, G.A., Golunova, M.A., van Reenen, D.D., 2012. Experimental and petrological constraints on local-scale interaction of biotite-amphibole gneiss with H_2O-CO_2-(K, Na)Cl fluids at middle-crustal conditions: example from the Limpopo Complex, South Africa. Geoscience Frontiers 3, 829–841.
Shmulovich, K.I., Graham, C.M., 1996. Melting of albite and dehydration of brucite in H_2O–NaCl fluids to 9 kbars and 700–900 °C: implications for partial melting and water activities during high pressure metamorphism. Contributions to Mineralogy and Petrology 124, 370–382.
Shock, E.L., Helgeson, H.C., 1988. Calculation of thermodynamic and transport properties of aqueous species at high pressures and temperatures: correlation algorithms for ionic species and equation of state predictions to 5 kb and 1000 °C. Geochimica et Cosmochimica Acta 52, 2009–2036.
Spear, F.S., 1993. Metamorphic Phase Equilibria and Pressure-Temperature-Time Paths. Mineralogical Society of America Monograph, Washington.
Srikantappa, C., Raith, M., Spiering, B., 1985. Progressive charnockitizationof a leptynite–khondalite suite in southern Kerala, India—Evidence for formation of charnockites through decreasein fluid pressure? Journal of Geological Society of India 26, 859–872.
Stähle, H., Raith, M., Hoernes, S., Delphs, A., 1987. Element mobility during incipient granulite formation at Kabbaldurga, Southern India. Journal of Petrology 28, 803–834.
Thompson Jr., J.B., 1959. Local equilibrium in metasomatic processes. Researches in Geochemistry 1, 427–457.
Touret, J.L.R., Huizenga, J.M., 2011. Fluids in granulites. In: van Reenen, D.D., Kramers, J.D., McCourt, S., Perchuk, L.L. (Eds.), Origin and Evolution of Precambrian High-Grade Gneiss Terrains, with Special Emphasis on the Limpopo Complex of Southern Africa. Geological Society of America Memoirs, pp. 25–37.
Touret, J.L.R., Nijland, T.G., 2013. Prograde, peak and retrograde metamorphic fluids and associated metasomatism in upper amphibolite to granulite facies transition zones. In: Harlov, D.E., Austrheim, H. (Eds.), Metasomatism and the Chemical Transformation of Rock. The Role of Fluids in Terrestrial and Extraterrestrial Processes. Springer, pp. 415–469.
Yardley, B.W.D., Graham, J.T., 2002. The origins of salinity in metamorphic fluids. Geofluids 2, 249–256.
Yund, R.A., Tullis, J., 1983. Subsolidus phase relations in the alkali feldspars with emphasis on coherent phases. Feldspar Mineralogy (2nd Edition). Reviews in Mineralogy 2, 141–176.
Zhu, C., Sverjensky, D.A., 1991. Partitioning of F-Cl-OH between minerals and hydrothermal fluids. Geochimica et Cosmochimica Acta 55, 1837–1858.
Zhu, C., Sverjensky, D.A., 1992. F-Cl-OH partitioning between biotite and apatite. Geochimica et Cosmochimica Acta 56, 3435–3467.